

AUG 21 1998

SANDIA REPORT

SAND98-1461
Unlimited Release
Printed July 1998

SAND - - 98-1461

Development and Evaluation of Sealing Technologies for Photovoltaic Panels

RECEIVED

SEP 01 1998

JST

S. Jill Glass, F. Michael Hosking, Paul M. Baca, William F. Hammetter,
Scott T. Reed, Robert R. Dubois, Peter G. Stromberg, Thomas Voth,
Steven E. Gianoulakis, Edward L. Hoffman, Scot Albright

Prepared by
Sandia National Laboratories
Albuquerque, New Mexico 87185 and Livermore, California 94550

Sandia is a multiprogram laboratory operated by Sandia Corporation,
a Lockheed Martin Company, for the United States Department of
Energy under Contract DE-AC04-94AL85000.

Approved for public release; further dissemination unlimited.



Sandia National Laboratories

MASTER

DISTRIBUTION OF THIS DOCUMENT IS UNLIMITED

Issued by Sandia National Laboratories, operated for the United States Department of Energy by Sandia Corporation.

NOTICE: This report was prepared as an account of work sponsored by an agency of the United States Government. Neither the United States Government nor any agency thereof, nor any of their employees, nor any of their contractors, subcontractors, or their employees, makes any warranty, express or implied, or assumes any legal liability or responsibility for the accuracy, completeness, or usefulness of any information, apparatus, product, or process disclosed, or represents that its use would not infringe privately owned rights. Reference herein to any specific commercial product, process, or service by trade name, trademark, manufacturer, or otherwise, does not necessarily constitute or imply its endorsement, recommendation, or favoring by the United States Government, any agency thereof, or any of their contractors or subcontractors. The views and opinions expressed herein do not necessarily state or reflect those of the United States Government, any agency thereof, or any of their contractors.

Printed in the United States of America. This report has been reproduced directly from the best available copy.

Available to DOE and DOE contractors from
Office of Scientific and Technical Information
P.O. Box 62
Oak Ridge, TN 37831

Prices available from (615) 576-8401, FTS 626-8401

Available to the public from
National Technical Information Service
U.S. Department of Commerce
5285 Port Royal Rd
Springfield, VA 22161

NTIS price codes
Printed copy: A04
Microfiche copy: A01



DISCLAIMER

**Portions of this document may be illegible
in electronic image products. Images are
produced from the best available original
document.**

Development and Evaluation of Sealing Technologies for Photovoltaic Panels

S. Jill Glass* and **F. Michael Hosking***
Materials Joining Department

Paul M. Baca
Catalysis and Chemical Technologies Department

William F. Hammetter
Materials Processing Department

Scott T. Reed
Ceramic and Glass Processing Department

Robert R. Dubois
Mechanical Engineering Department

Peter G. Stromberg
Guidance and Control Department

Thomas Voth and Steven E. Gianoulakis
Thermal Sciences Department

Edward L. Hoffman
Engineering and Manufacturing Mechanics Department

Sandia National Laboratories
P.O. Box 5800
Albuquerque, NM 87185-0367

and

Scot Albright*
Golden Photon Technologies
4545 McIntyre St.
Golden, CO 80403

Abstract Follows

* Primary authors to contact for further information.

*Presently at Global Solar Energy, 12401 W. 49th Ave., Wheat Ridge, CO 80033.

Abstract

This report summarizes the results of a study to develop and evaluate low temperature glass sealing technologies for photovoltaic applications. This work was done as part of Cooperative Research and Development Agreement (CRADA) No. SC95/01408. The sealing technologies evaluated included low melting temperature glass frits and solders. Because the glass frit joining required a material with a melting temperature that exceeded the allowable temperature for the active elements on the photovoltaic panels a localized heating scheme was required for sealing the perimeter of the glass panels. Thermal and stress modeling were conducted to identify the feasibility of this approach and to test strategies designed to minimize heating of the glass panel away from its perimeter. Hardware to locally heat the glass panels during glass frit joining was designed, fabricated, and successfully tested. The same hardware could be used to seal the glass panels using the low temperature solders. Solder adhesion to the glass required metal coating of the glass. The adhesion strength of the solder was dependent on the surface finish of the glass. Strategies for improving the polyisobutylene (PIB) adhesive currently being used to seal the panels and the use of Parylene coatings as a protective sealant deposited on the photovoltaic elements were also investigated. Starting points for further work are included.

Contents

Objectives.....	6
Background.....	6
Approach.....	7
Thermal Modeling	7
Stress Modeling.....	8
Glass Frit Joining.....	9
Solder Joining.....	10
Polyisobutylene (PIB) Adhesive Improvements	12
Parylene Coatings.....	12
Hardware	13
Summary.....	14
Starting Points for Future Work	15
Outstanding Issues.....	15
References	16

Figures

1 Golden Photon Solar Panel	6
2 Panel Sealing Arrangement	8
3 Glass Panels Bonded with Johnson Matthey Glass Frit ($T_{mp} \sim 325^\circ C$)	10
4 Position of Thermocouples	14

Tables

1 Temperature of the glass panel	8
2 Lap shear strength of soldered glass to glass joints.....	11

APPENDICES

APPENDIX A - Thermal Modeling	17
APPENDIX B - Thermal Modeling	24
APPENDIX C - Stress Modeling.....	36
APPENDIX D - Polyisobutylene (PIB) Adhesive Improvements	43
APPENDIX E - Hardware Drawings	47

Objectives

The overall objective of this Cooperative Research and Development Agreement (CRADA) was to develop an improved joining technology for photovoltaic modules in order to ultimately enhance and accelerate product penetration in the marketplace.

The specific technological objectives were:

1. Optimize the solder bonding technology for joining plate glass for photovoltaic modules;
2. Identify alternative bonding technologies;
3. Transform science solutions into manufacturing practice.

Background

Golden Photon, Inc. (GPI) has demonstrated the field use of CdTe-based Photovoltaic modules. The primary advantages of the technology are 1) the simplicity, and therefore low-cost of the processing equipment; 2) the forgiving nature of the active semiconductor materials (CdS and CdTe); and 3) the resulting low processing costs. A typical panel is shown in Fig. 1.

The primary obstacle to obtaining the desired field life of 20 years or greater, is that the active semiconductor material in unencapsulated modules degrades with time in the presence of excessive humidity. Expected field life is therefore directly related to the permeability of water into the module through the edge seal. The total measured permeability for the current design is characterized by exposure to 85°C, 85% RH for extended periods. The total weight of water per year per lineal foot of edges is the figure of merit. The present value is 0.56-0.73 g of water per year per lineal foot of edge.¹ To increase the life of the module in the field, to improve the confidence of the lifetime prediction, and to reduce or eliminate the desiccant that is presently used to reduce the moisture content of the module, a significant reduction in permeability of the module is required. The goal of the project was a 100-fold reduction of water permeability per year per lineal foot of edge at 85°C, 85% RH. The resulting module must also pass "Recommended Practice for Qualification of Photovoltaic Modules," prepared by IEEE Standards Coordinating Committee 21, Photovoltaics. This includes thermal cycling (dry and humidity-freeze), hail impact tests, twist tests, flexion tests, and various loading tests.²

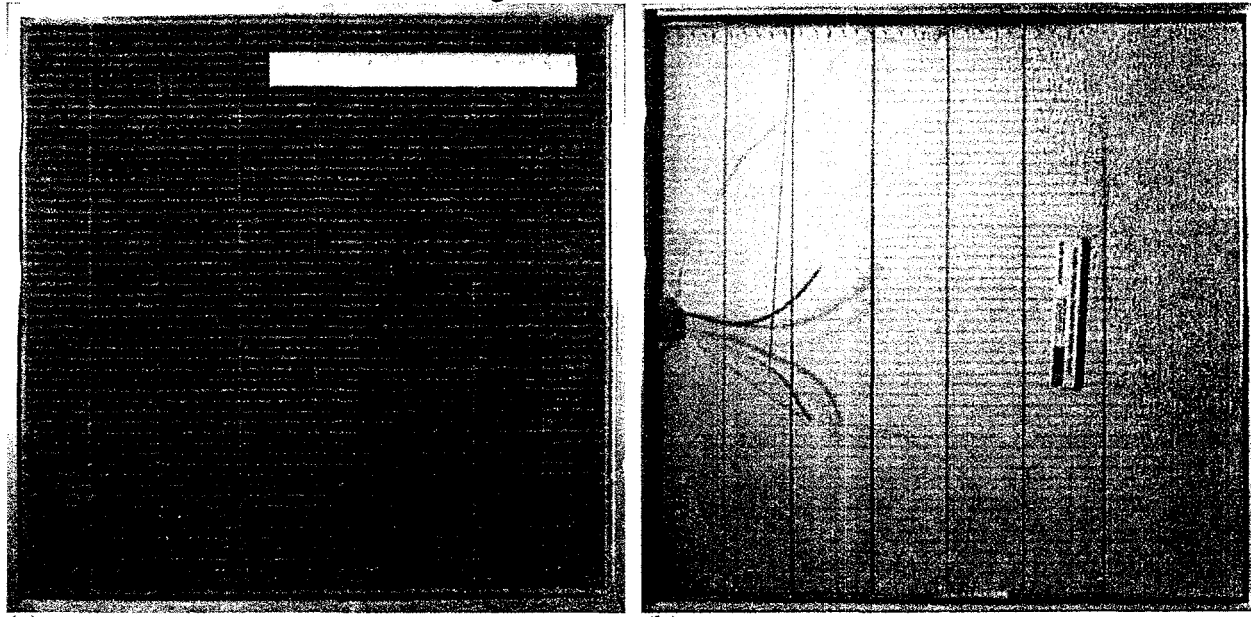


Fig. 1. Golden Photon solar panel with aluminum frame. The dimensions are 24"x24". The design is from the early stages of the project and is sealed with a polyisobutylene (PIB) adhesive. (a) Front of panel (b) Rear of panel. Loose desiccant, which is beige, is present on the right side of the panel.

Whatever sealing materials or techniques are used, they must be compatible with the soda lime glass front and rear panels, the aluminum frame around the panels, and the various photovoltaic materials (Ni-Cr, carbon, CdTe, CdS). The sealing technology should allow the elimination of the desiccant, ease of assembly, and a fifteen-twenty year life span in a hot and humid environment (extrapolated from an 85°F, 85% RH test environment).

A small initiative began in the summer of 1994 demonstrated that glass could be bonded with a low temperature solder using existing Sandia technology. Once the CRADA was in place, a meeting was held at Golden Photon (March 22, 1996) to brainstorm and identify alternative sealing technologies. The main constraint on the sealing technology is that at 0.5" (approx.) from the edge of the glass panel the temperature cannot exceed ~250°C because of the presence of a graphite coating on the CdTe layer. There is approximately 10 mil (250 μm) clearance between the glass panels. This space is needed to accommodate the active elements and a crimped bus bar.

When the project began, the moisture problem was being minimized by including loose desiccant between glass panels that were sealed by Polyisobutylene (PIB). During the project with Golden Photon, the loose desiccant was replaced by a desiccant canister that was attached to the back glass panel. Access for the desiccant was through a 5/16" hole.

Approach

The first task was to propose and evaluate ideas for providing a controlled environment for the CdTe and CdS films on Golden Photon's photovoltaic panels. Ideas included providing a hermetic seal between the two glass plates by improving Golden Photon's existing technology (polyisobutylene (PIB) adhesive), implementing new sealing technology, replacing the back glass plate with a metal foil that would be hermetically bonded to the front glass plate, and coating the active elements with a transparent coating in conjunction with the existing sealing technology. After our initial evaluations, we pursued two approaches to reducing the exposure of the active elements to moisture. One was to hermetically bond glass plates together at low temperatures and the other was to use a polymer coating to cover the active elements. Both of the bonding approaches required that the glass temperature not exceed ~250°C at 0.5 inches in from the edge of a 24"x24" panel. The first bonding approach used a low temperature glass frit in conjunction with localized heating to prevent the glass from exceeding the critical temperature away from the joint. The second bonding approach utilized a low temperature solder (T_{mp} ~210°C) on metal-coated glass. In support of these approaches we used thermal transport and stress simulation codes to determine what processing parameters, geometries, and sizes would allow us to stay within the desired temperature range of ~250°C. Hardware that will allow localized heating of the glass frit and the low temperature solder was designed, manufactured, and tested. Hermeticity testing of the sealed panels was not completed. Each area of the study is summarized in the remainder of the report starting with the thermal and stress modeling, followed by the evaluation of the glass, solder and organic bonding, materials, and finishing with a description of the hardware used for localized heating of the glass panels. Further details about some of these studies can be found in the Appendices.

Thermal Modeling

Details of the thermal modeling effort can be found in two memos that are Appendices A and B of this report. A schematic of the geometry of the panel sealing arrangement that was used for the modeling is shown in Fig. 2.

The thermal response of the part for localized heating was modeled as a function of different heating rates (25 and 50°C/min) and hold times (0, 2 and 5 min) at the melting temperature for a fixed glass frit melting temperature of 430°C (See APPENDIX A). For these cases, thermal energy was supplied to the periphery (all four sides) of the glass panel. Results indicate that the maximum temperature would be exceeded in the critical area with traditional glass frits that melt in the range of 430°C. One solution for this would be to increase the distance between the edge of the glass panel and where the active elements are located from

0.5 to 1.0 inches. This solution was resisted by the manufacturer because of the loss of element area and the resulting loss in power output.

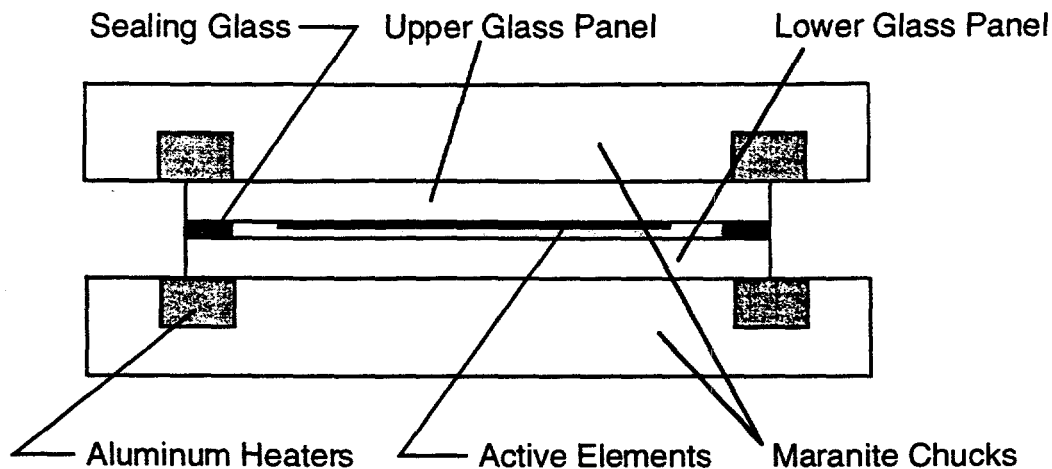


Fig. 2. Schematic of the panel sealing arrangement.

The thermal analysis for 6" x 6" plates and 24" x 24" glass plates predicted similar results.

The situation in which parallel sides of the plate were heated sequentially was also modeled to determine if this reduced the absolute temperature in the glass and the thermal gradient (See APPENDIX B). This modeling was done for a glass frit with a melting temperature of 350°C. The staggered heating with a hold time of 0, 0.5 or 2P (where P=ramp-up, dwell, and cool-down) between when the first and second set of heaters are turned on produced substantial decreases in the maximum temperature achieved in the corner of the glass panels, 0.5 inches from each edge as shown in Table 1.

Table 1. Temperature of the glass panel, 0.5 inches from each edge, under different processing conditions.

Dwell Time	25°C/min, 0P Hold	25°C/min, 0.5P Hold	50°C/min, 0P Hold	50°C/min, 0.5P Hold
0 min	274°C	211°C	244°C	163°C
2 min	290°C	223°C	271°C	203°C
5 min	306°C	241°C	297°C	227°C

For example, this modification produced a 63°C reduction in the temperature for a heating rate of 25°C/min, a dwell time of 0 min and a hold of 0.5 P. There were no advantages to using a hold time greater than 0.5 P, and this would only increase the total production time.

Results were compared to actual temperature profiles measured using thermocouples at various positions on the glass plates.

Stress Modeling

Details of the stress analysis can be found in a memo that is included in the APPENDIX C of this report. Using the output from the thermal modeling, the position and magnitude of the maximum tensile stress due to thermal gradients were modeled assuming that the glass was elastic. The maximum tensile stress of ~39.8 MPa (5800 psi) is located in the region of the highest thermal gradient when a glass frit melting temperature of 430°C was used. The highest stress occurs when the temperature at the corner of the glass panel is 369°C. Although this stress exceeds the strength that is usually used as the design stress for glass, the stress is transient, and therefore may not produce cracking in the manner that it would under sustained

loading when subcritical crack growth can occur. It is also worth noting that the maximum stress occurs in a region away from the edge of the glass plate. This is beneficial because the worst flaws are usually located at the edges of the plate where cutting damage occurs. If the maximum stress were located in this region, cracking would be more likely. The stress analysis for 6"x6" plates and 24"x24" plates produced similar results in terms of the magnitude and position of the maximum tensile stress.

Glass Frit Joining

Our initial efforts were with a Plasmaco glass frit with a melting temperature of 430°C.* Based on the initial thermal modeling results we chose to evaluate glass frits with lower melting temperatures than those available using traditional glass frits.³ A developmental frit that has a good thermal expansion match with Corning 7059 glass was provided by Johnson Matthey.[†] It is composed of compounds of lead, zinc, copper and manganese. The glass frit is applied as a slurry to the glass and then put under a heat lamp to remove the volatiles. It is then heated to 140°C to remove the organic binder. TGA/DTA results indicate that binder burnout is complete by 140°C. Its melting temperature was specified as 350°C but it appeared to melt at 330°C during initial tests. It produced a bubble-free joint at the specified melting temperature using conventional oven heating of 1"x1" coupons. At higher temperatures (380°C), there appeared to be some degradation of the glass, with the frit becoming less viscous.

The melting of the glass frit also appeared to be sensitive to the heating rate. It appeared to crystallize during heat-up at a ramp rate of 5°C/min. This crystallization behavior appears to cause it to set until much higher temperatures are reached (>400°C). These temperatures are unsuitable in terms of keeping the glass away from the edges at temperatures below ~250°C. When a ramp rate of ~50°C/min was used for 6"x6" no crystallization was observed and the glass melted at temperatures in the range of 320-330°C. Quick thermal excursions through temperature ranges where crystal phases nucleate and grow should limit or prevent crystal growth. The glass also contracts significantly during melting, drawing in glass from the surrounding regions, and in some cases causing a columnar structure to form that may be detrimental in terms of the hermeticity. There appear to be several phases in the glass. Some of these may simply be fillers to control the coefficient of thermal expansion (CTE).

The glass frit was successfully melted and used to bond two 6"x6" pieces of float glass together using the hardware built to produce localized heating. All four heaters were energized. The glass melted and flowed slightly out of the joint in some regions when the heater elements set-point was approximately 385°C. The glass in the corner (1/2 each from each edge) reached a maximum temperature of 257°C at a time of 700 seconds, 200 seconds after the glass melted. There were small cracks along the edge of one of the glass plates and perpendicular to that edge as shown in Fig. 3. These cracks most likely formed during cooling. This problem might be eliminated by tuning the heating and cooling profiles. Active cooling may help reduce the corner temperatures and would also provide the added benefit of speeding up the process. Cracking can also be minimized by ensuring that the edges of the glass plate are relatively flaw free. This can be achieved by careful machining and subsequent finishing and annealing.

* Schott Glass frit from Plasmaco that replaces Schott G017-334. It has a high PbO content and a density of 4.8 g/cc. Assumed to be ~60% PbO, 40% SiO₂.

† JM8400-045 Sealing Glass Paste, Lot 042363. Johnson Matthey Electronics, 10080 Willow Creek Rd., San Diego, CA 92131. (619 566-9510).

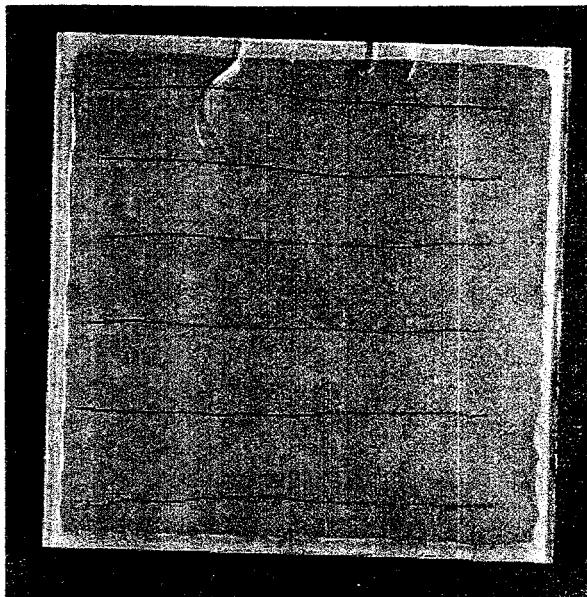


Fig. 3. Photograph of the 6"x6" glass panels bonded with Johnson Matthey glass frit ($T_{mp} \sim 325^\circ\text{C}$) in which the heater set-point was $\sim 400^\circ\text{C}$. The horizontal lines are ink lines drawn to distinguish the top plate of glass from the bottom plate in case of catastrophic fracture during processing.

Solder Joining

Initial tests indicated that soda-lime-silicate glass could be wetted with 63Sn-37Pb ($T_m = 183^\circ\text{C}$), 60Sn-40Pb ($T_m = 183-188^\circ\text{C}$), and 80In-15Pb-5Ag ($T_m = 148-149^\circ\text{C}$) solders after sputter coating the glass with 0.15 μm Cr - 0.15 μm Pd - 2.5 μm Au, respectively.^{4,5} Sessile drop tests conducted without flux in nitrogen and vacuum at 205-210°C indicated that the SnPb solder gave the best wetting results. A fluxless solder is desirable because the absence of chemical flux residues in the panel after soldering eliminates potential long term corrosion problems. Some fluxes are more of a problem than others.

Glass-solder-glass lap joints were made and used for microstructural analysis. Tests were also done in helium to determine the feasibility of processing the joint in an atmosphere that was inert and could be used to detect seal leaks after soldering. Lap shear specimens were made from stainless steel soldered to the coated glass. (The strength of the steel-glass bond was of interest initially because in the original design there was a stainless steel spacer between the two glass panels. This was subsequently eliminated.) The average shear strength for seven specimens was 11 MPa (1600 psi). The strength ranged from 7.6-14.7 MPa.⁶ The stronger joints appeared to have more solder adhering to the glass. Weaker joints tended to show a web-like coverage of the glass by the solder.

Scanning electron microscopy examinations of cross sectioned glass-to-glass joints showed good coverage of the glass by the solder. The solder itself appears to be somewhat inhomogeneous with three major phases identified by Energy Dispersive Spectroscopy (EDS). There is a Pb-rich phase, a plate-like Sn-Au intermetallic phase and a Sn-rich phase. There appears to be some segregation of the Pb-rich phase in the middle of the joint and segregation of the Sn-Au intermetallic in layers. This segregation may contribute to weakening of the joint. There was some evidence to suggest that failure of the joint occurs along the segregated layers. We believe that the presence of significant amounts of the Sn-Au intermetallic was due to too thick a Au coating on the glass metallization. We used 2.5 μm for initial attempts but used 1 μm for our next set of specimens. A reduction in the amount of gold would reduce the amount of the Sn-Au intermetallic phase with a corresponding increase in the strength of the joint.⁷ Results, although limited, indicated that thinner Au coating was better. There was less intermetallic in the joint.

The gold coating option was not pursued further because our focus shifted to soldering to glass coated using Golden Photon's current process. They use a 26Ni-74Cr coating that is 75-100Å thick. It is deposited on the edge deleted surface on the perimeter of the glass panel in a vacuum furnace. Subsequently a 1 µm thick layer of Sn is deposited on top of the Ni-Cr layer.

Ni-Cr coated glass coupons were tested to determine whether the existing coating was conducive to soldering. The low temperature solders wet the coating well both for as-received and edge-deleted glass. Bonded coupons were produced that appeared to have good integrity, although the solder may not have adhered in all locations due to the roughness of the glass surface. The smooth surfaces seemed to have ~70-80% coverage whereas the rough surfaces had ~5-30% coverage when a flux was used with the solder. On the smooth surfaces without a flux, using an inert atmosphere, the coverage was ~100%. Three different coating thicknesses of Ni-Cr were evaluated (100, 1000 and 10,000Å), using coatings produced in Sandia's Thin Film and Brazing Lab. There was no evidence of the dewetting or dissolution that we had initially observed. This may be because the initial samples were produced using Golden Photon's existing process and the surface coverage on these coupons may not have been complete.

Shear strengths were measured for different surface preparations (rough vs. smooth), different glass coating thicknesses, and different soldering conditions at a test rate of 0.01 mm/s. The results are shown in Table 2.

Table 2. Lap shear strength of soldered glass to glass joints.

Soldered Test Sample	Smooth/Smooth Strength (psi)	Smooth/Rough Strength (psi)	Comments
Au/Ni/Steel-to Cr/Pd/2.5 µm Au/Glass	1580 ±400		210°C/N ₂ No Flux
Glass-Au/Ni/Steel-Glass (Cr/Pd/1.0 µm Au)	2200		210°C/He No flux
Glass-Glass (Cr/Pd/1.0 µm Au)	2400		210°C/He No flux
Glass-Glass (GP-NiCr/Sn Baseline)	1675±180 (~50% bonded)		220°C/R-flux N ₂ Cover
Glass-Glass (GP-NiCr/Sn Baseline)		300 (~20% bonded)	220°C/R-flux N ₂ Cover
Glass-Glass (SNL-NiCr/Sn: 100 Å/1.5 µm)	3335±85	2139±561	220°C/R-flux N ₂ Cover
Glass-Glass (SNL-NiCr/Sn: 1,000 Å/1.5 µm)	3342±404	1827±218	220°C/R-flux N ₂ Cover
Glass-Glass (SNL-NiCr/Sn: 10,000 Å/1.5 µm)	3031±531	1309±579	220°C/r-flux N ₂ Cover
Glass-Glass (SNL-NiCr/Sn: 100 Å/1.5 µm)	2690 (~90% bonded)	690 (~50% bonded)	220°C/R-flux Air

Test samples were processed with a nitrogen inerted table-top reflow machine, using a reflow profile of 220°C peak topside temperature and a four minute processing time (from room temperature to final peak temperature soak). A rosin-based flux was lightly applied to the 60Sn-40Pb (wt. %) solder preforms before soldering to accommodate the partially inert conditions of the process. The samples were uniformly heated in this arrangement. The shear strengths of solder joints for smooth-to-smooth surfaces were in the range of 3000-3300 psi, with failures primarily in the glass pieces. The smooth-to-rough joints were in the range of 1300-2100 psi and generally failed between the glass and solder interface on the "rough" side of the joint. The lower strength of the solder bond on the rough (edge-deleted) surface was probably due to

the removal of the SnO_2 film during the edge-delete operation and an uneven NiCr/Sn coating thickness, resulting from the rough profile of the edge-delete surface. SnO_2 is normally deposited on the glass to promote adhesion of subsequent "active" layers. The oxide film was removed during the edge delete process, prior to deposition of the NiCr and Sn coatings. Its absence could reduce the overall adhesion of the succeeding films. It is also likely that the edge-delete machining process introduced surface flaws that further contributed to the reduced joint strengths. A mask could be put down to protect the SnO_2 and NiCr coatings during subsequent coatings processes (CdS, CdTe, graphite, etc.).

The SnO_2 effect on bond strength was investigated during the next round of testing at Sandia. Individual 1"x1" NiCr/Sn coated glass coupons, without SnO_2 between the NiCr and glass, were fabricated. Shear test specimens were soldered using the processing and test conditions used to evaluate the SnO_2 coated glass substrates with 100 Å NiCr and 1.5 μm Sn. The resulting smooth/smooth shear strengths were 2860 psi \pm 278, comparable to the SnO_2 coated samples. The lower strengths of the roughened samples appear to be caused more by the induced surface flaws and uneven coating of the NiCr and Sn layers.

Another important investigation was to determine the soldering requirements for scaling up to the 6"x 6" test configuration. Four test plates were directly metallized with 100 Å NiCr and 1.5 μm Sn around their outer 0.5" perimeter. Prototype soldering with the resistance heating device described in the "Hardware" section (see below) was planned. The project ended before these experiments could be conducted.

Polyisobutylene (PIB) Adhesive Improvements

Polyisobutylene (PIB)[‡] adhesive is the sealing technology that was being used at Golden Photon during the duration of this project. When the front and back glass plates are pressed together the PIB is at 125°F and the glass is at room temperature. There is an applied pressure of 10 psi on a 1" band around the plates. The only cleaning prior to the PIB application is to vacuum off any ground glass from the edge delete surface of the front glass panel on which the active elements are deposited. Several suggestions were made for improving the level of performance of the PIB sealing technology (APPENDIX D). Many of these suggestions related to the surface preparation of the glass prior to the application of the PIB. The PIB contains glass beads that could serve as leakage paths between the PIB and the glass beads. The use of a coupling agent should improve the bonding between the PIB and the glass plate if it is not already incorporated in the adhesive. Information about the coupling agent, as well as the actual glass bead loading of the adhesive, were proprietary. One way to minimize leakage paths due to the presence of the glass beads would be to use PIB-3, which contains no beads. Other butyl compounds that can match PIB's moisture permeability may offer better wet-out and adhesion to the glass. One example is polyvinyl butyral, which is used extensively in glazing applications. Urethanes, which initially have higher moisture permeability, but then couple with water molecules over time, may retard permeability.

Parylene Coatings

The use of Parylene[§] coatings as a transparent sealant deposited on the photovoltaic elements was proposed for evaluation late in the project. Parylene is a vapor-depositable polymer that can be deposited under roughing pump pressures with the substrates at room temperature. The basic member of the Parylene family, Parylene N, is poly-para-xylylene, a completely linear, highly crystalline material. Parylene provides a conformal coating due to the vapor phase deposition, and can be formed as continuous coatings with thicknesses from submicron to tens of microns. Six test panels (~2"x2") with active elements were coated with Parylene N and Parylene D. Parylene N and Parylene D have moisture vapor transmissions at 90% RH, 37°C of 1.5 and 0.25 g-mil/100 in²-day) respectively. Test panels were sent to Golden Photon in Aug. 1997 for testing in the 1000 hr test at 85°C in 85% RH. The intention was to test them for their I-V output and then compare the values to uncoated panels. Testing was not completed because of the closure of Golden Photon's facilities.

[‡] ADCO's PIB-7 that contains 0.010" diameter glass beads.

[§] Parylene Conformal Coatings, Specialty Coating Systems, Union Carbide Corp, 5707 W. Minnesota St., Indianapolis, IN 46241.

Hardware

Various options for locally heating the glass on the perimeter of the panel were evaluated including lasers, high intensity lamps, induction heating, and microwave heating. Lasers had been investigated at Sandia for sealing flat panel displays.^{8,9,10} We decided to pursue heating with a device with embedded heating elements, similar in design, but simpler, than equipment constructed for the National Center for Advanced Information Components Manufacturing (NCAICM) Project.

We designed, built, and tested hardware that allowed heat to be applied in a very localized region around the perimeter of two 6"x6" plates of glass. The chuck was constructed of Maranite thermally insulating block, 17.78 cm (7 inches) on a side and 1.27 cm (0.5 inches) thick. Thermal energy is supplied to the two stacked glass panels via an aluminum electrical resistance heating element embedded in the Maranite. Drawings of the chuck are provided in APPENDIX E. The hardware can be used for bonding with glass frits, where localized heating is a necessity because the frit melting temperature (T_{mp} ~350°C) is higher than the critical temperature of ~250°C, and for bonding with low temperature solders where the temperature of the glass is not critical because the solder melting temperature is well below 250°C. Both glass plates are heated using heating elements on the top and the bottom of the heating fixture. The hardware was also constructed such that heating of alternate pairs of sides was possible.

Initial tests were used to measure the temperature profile in the glass without the glass frit. The heating rate was ~35°C/min to 220°C. Temperature vs. time was monitored for the nine thermocouples in the interior of the glass plate and for one on the edge of the glass plate for different heater element setpoints (250°C, 350°C, 400°C). There was a temperature lag between the elements and the edge thermocouple of ~ 80°C. Therefore with a set-point of 350°C, the edge is hot enough to melt the low temperature solder, and at a set-point of 400°C, the edge is just hot enough to melt the low-melting glass frit from Johnson-Matthey (T_{mp} ~325-350°C).

In one test the glass fractured catastrophically. The fracture origin was in the region approximately 1.5" in from the edge, where FEA had predicted high stress. Examination of the glass fracture surface indicated that the failure stress was approximately 4100 psi, consistent with Ed's stress predictions. An applied weight and centering pins may have contributed to the problem because of the constraint they provided when the glass was expanding during heating. They were eliminated for future runs and subsequent tests were conducted without catastrophic glass fracture.

For a run in which the Johnson Matthey frit melted and bonded the two glass panels, the approximate positions of the nine thermocouples and their temperatures are shown in Fig. 4. The heater setpoint was 400°C and the temperature at the edge of the glass was 318°C, very close to the temperature where melting occurs for the Johnson Matthey frit.

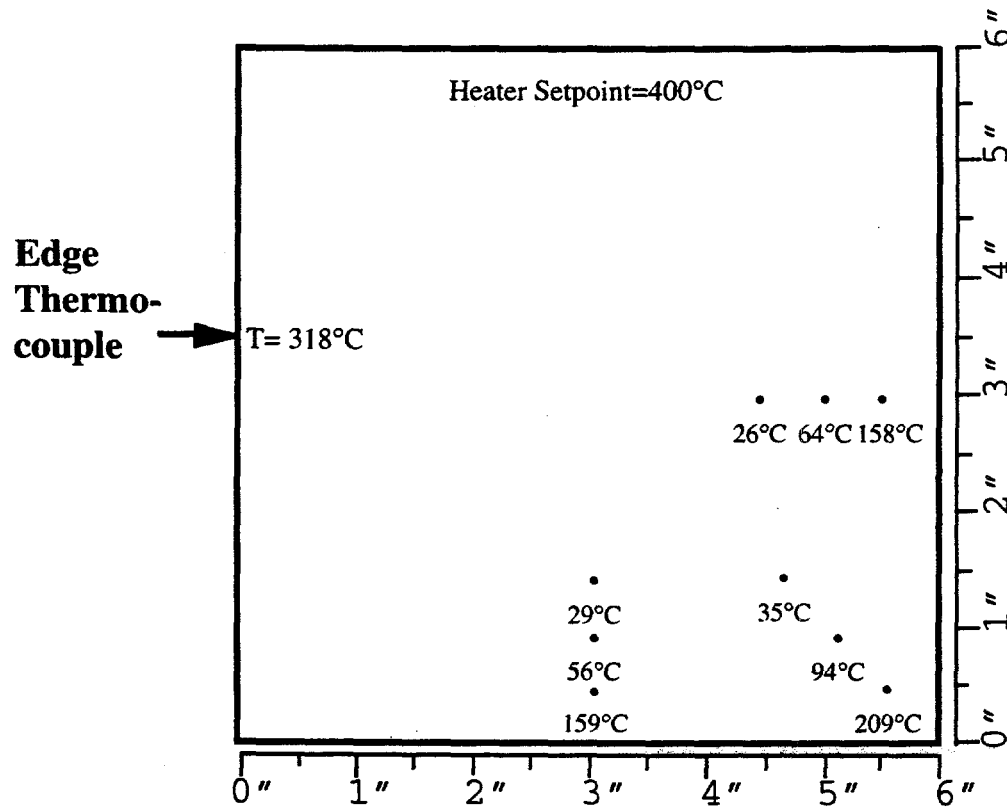


Fig. 4. Position (•) of nine thermocouples used to monitor the glass temperature and the thermocouple used to monitor the temperature at the edge of the glass.

Summary

Two different glass sealing technologies have been evaluated for bonding glass panels for solar panel applications. One utilizes low temperature solders to bond the glass after it has been coated with thin metal coatings and the other utilizes low melting glass frits. Thermal modeling and stress modeling indicated that a localized heating approach could be used to achieve a high enough temperature to melt the glass frit or solder without allowing the glass 0.5" from the edge to exceed the maximum temperature limit (~250°C) of the active elements bonded to the glass. A staggered heating approach in which the four heating elements on the perimeter were heated as parallel pairs with a delay time in between when the first and second set of elements were turned on indicated that the maximum temperature in the corner of the glass panels could be reduced even further. Tensile stresses on the order of 39 MPa (7800 psi) were modeled for the predicted thermal gradients in the glass. Although this stress level is high, it is a transient stress and occurs in a region away from the edge of the glass where the glass is expected to be weakest. An active cooling approach might minimize the thermal gradients that lead to these stresses and would also reduce the processing time. Hardware was constructed that allows localized heating of the glass. Trials in which a glass frit with a melting temperature of ~325°C was used were successful in bonding the glass together without exceeding the 250°C temperature limit. Some cracking of the edge of the glass was observed but this could be minimized by finishing the edges of the glass to reduce the damage in the cut edge and thereby increase the strength of the glass. Cracking could also be eliminated by tuning the heating and cooling schedules.

Starting Points for Future Work

- Optimize bonding with glass frit by tuning the heating and cooling profiles of the localized heating hardware.
- Explore the use of active cooling in the center of the plate to maintain the glass temperature below 250°C and to reduce the thermal gradients during cooling.
- Change the configuration of the heaters in the corner to reduce the temperature and temperature gradient in the glass adjacent to the corners.
- Screen print the glass frit (or solder alloy) onto the plate glass to achieve reproducible and uniform thickness.
- Optimize bonding with low temperature solder and Ni-Cr coated glass.
- Test hermeticity of glass frit and solder bonds.
- Heat 6"x6" panels with CdTe and CdS coatings in the localized heating hardware and check afterwards whether efficiency has been lost.
- Conduct stress modeling to determine what stresses the joints and glass see in service.

Outstanding Issues

- Alternatives to measuring the weight gain of the desiccant as the quantifier of permeability need to be identified.¹¹
- The effects of the edge deletion process on both coating for soldering and how the process may introduce mechanical flaws that contribute to glass breakage during heating and cooling need to be understood.
- Environmental Protection Agency issues relating to the solder and glass frit bonding materials.
- The temperature and time that can be sustained by the active elements depends on the environment during bonding (it ranges from 250°C for 10 min in inert atmosphere to 150°C for 1 hr in air).
- The space available between edge of plate and the active elements may be critical. If this was larger than the current value of ~0.5", our ability to stay below the critical temperature would be enhanced.

References

- ¹ S. Albright, AMMPEC Presentation Overview, Low Temperature, Hermetic Encapsulation Packaging for Photovoltaic Modules, Feb. 3, 1994.
- ² Aug. 12, 1996 Semiannual report from Scot Albright's to Jeff Bullington at AMMPEC.
- ³ C. J. Hudecek, Sealing Glasses, pp. 1069-1073, Ceramics and Glasses, Vol. 4, ASM Engineered Materials Handbook, 1991.
- ⁴ July 8, 1994 memo from Mike Hosking to Jill Glass and Dick Brow, Golden Photon Info.
- ⁵ July 11, 1995 memo from Mike Hosking, 1831, to Bill Hammetter, 1846, Golden Photon Glass Bonding Information.
- ⁶ July 27, 1994 memo from D. T. Schmale, 1832, to Jill Glass, 1845, Shear Strength of Stainless Steel-Glass Solder Joints.
- ⁷ August 3, 1994 memo from S. Jill Glass, 1845, to W. F. Hammetter, 1846, Shear Testing and Fracture Surface Evaluation of Stainless Steel-Glass Joints for the Golden Photon Program.
- ⁸ March 17, 1994 memo from R. S. Chambers, 1561 to L. Kovacic, 2476, Some Rough Computations Demonstrating the High Tensile Stresses Expected When Laser Sealing Flat Glass Panels - NCAICM Project 299322135.
- ⁹ May 5, 1995 memo from R. S. Chambers, 1517, to Distribution, Geometric Modeling Considerations in Analyzing the Thermal residual Stresses in an Oven Sealed Flat Panel Display.
- ¹⁰ Nov. 6, 1995 memo from R. S. Chambers to Distribution, Residual Stresses Generated in a Glass Panel when Subjected to Internal Vacuum.
- ¹¹ Dec. 4, 1996 memo from P. M. Baca to S. J. Glass, Quantification of Moisture in Golden Photon Panels.

APPENDIX A

May 17, 1996 memo from S. E. Gianoulakis and T. E. Voth, 9113 to S. J. Glass, 1845, Thermal Analysis of a Solar Panel Sealing Process for the Golden Photon CRADA.



Sandia National Laboratories

Operated for the U.S. Department of Energy by
Sandia Corporation

Albuquerque, New Mexico 87185-

date: May 17, 1996

to: S. J. Glass, MS 0333, Org. 1845

from: S. E. Gianoulakis and T. E. Voth, MS 0835, Org. 9113

subject: Thermal Analysis of a Solar Panel Sealing Process for the Golden Photon CRADA.

Introduction:

A thermal analysis has been performed to evaluate a solar panel sealing process in support of the Golden Photon CRADA. In the process investigated, a sealing glass is sandwiched between two rectangular glass panels (solar panels). The panels are heated on their periphery in order to melt the sealing glass, making a hermetic seal. The impetus for this study was concern that the sealing process may overheat and degrade the active elements which are deposited on one of the glass panels. Results indicate that, for realistic heating rates, and employing a sealing glass with a melting temperature of 430 °C, peak active element temperatures exceed 250 °C.

Process Description:

A thermal analysis has been performed for the solar panel and heater chuck arrangement shown schematically in Figure 1. The preliminary chuck design consists of a square Maranite thermally insulating block, 17.78 cm (7 inches) on a side and 1.27 cm (0.5 inches) thick. Thermal energy is supplied to the glass panels via an aluminum electrical resistance heating element embedded in the maranite. Together, the maranite insulating block and aluminum heater make up the chuck. The square glass panels considered in this study were 15.24 cm (6 inches) on a side and 0.3175 cm (0.125 inches) thick. The square heating element was 0.95 cm (0.375 inches) on a side and was located directly under the edge of the glass panel as shown in Figure 1. The chucks peripherally heat the glass panels and melt the sealing glass to form a hermetic joint. The sealing glass (Plasmaco frit) melts at a temperature of approximately 430 °C, which is substantially lower than the substrate glass (float glass) melting temperature. Active elements, which begin 12.7 mm (0.5 inches) in from the glass panel edge, must not exceed 250 °C for a period of longer than 10 minutes when processed in an inert environment, and 200 °C for 10 minutes in a 1000 ppm O₂ environment.

Analysis Description:

The finite element mesh of the chuck and glass panel assembly is shown in Figure 2. One-eighth symmetry was used to minimize mesh size. The sealing glass was not modeled as it should not significantly alter the substrate glass's thermal response. The relevant temperature-dependent

substrate glass and maranite thermophysical properties are given in Tables 1 and 2 respectively. Aluminum thermophysical properties are assumed to be temperature-independent and are $k = 177 \text{ W/m}\cdot\text{K}$, $c_p = 875 \text{ J/kg}\cdot\text{K}$ and $\rho = 2770 \text{ kg/m}^3$. The effect of the active elements, which would be incorporated in the actual upper glass panel, were ignored in this analysis (note that this provides a conservative estimate of panel temperature since the added thermal mass of the elements will reduce their maximum temperature slightly). Convective losses were assumed at all except symmetry surfaces. Symmetry surfaces were assumed to be adiabatic (insulated). Electrical heating of the aluminum strip was modeled by imposing the desired heater temperature history to the aluminum-glass panel interface. Various heater temperature ramp rates and hold ("soak") times were investigated to determine their influence on glass panel temperature at various positions from the periphery.

Analysis Results:

Ramp rates of 25 and 50 °C/min, and soak times of 0, 2 and 5 minutes were investigated to determine their influence on glass panel thermal response. In all cases, a maximum heater temperature of 430 °C was employed. Of particular interest is the resulting maximum active element temperature reached during the process. Since the active elements are not incorporated in the model, the maximum active element temperature is assumed to occur in the corner, on the surface of the glass panel where the elements would be attached in an actual assembly (see Figure 1). In the video conference of April 10, 1996 with Golden Photon and Sandia, the maximum separation distance between glass edge and active elements (the "dead-band") was specified as 1.27 cm (0.5 inches). Figure 3 shows the corner active element temperature histories for all ramp rate and soak time combinations investigated. It is evident from the figure that none of the processing histories result in maximum element temperatures less than 250 °C.

Figure 3 indicates that for realistic thermal processing parameters, maximum allowable active element temperatures are generally exceeded for elements placed 1.27 cm in from the glass panel edge. If, however, a wider dead-band is allowed, significant reductions in maximum active element temperatures can be achieved. Figure 4 shows the active element corner edge temperature histories for a dead-band of 25.4 cm (1 inch). The figure indicates that all cases (except the 25 °C/min, 5 minute soak case) result in maximum active element temperatures of less than 250 °C. Additionally, both the 50 °C/min, 0 and 2 minute soak processes result in maximum temperatures near or below 200 °C. It is anticipated that since the wider dead-band allows for lower heating rates, and hence reduced temperature gradients in the panel, thermally induced stresses (and hence cracking) can be minimized. This difference in thermal gradients induced in the glass for low and high heating rates is illustrated in Figure 5. Figures 5 (a) and (b) show the temperature distributions in the glass panel for the 25 °C/min, 0 minute soak and the 50 °C/min, 0 minutes soak cases respectively. The results of Figure 5 correspond to the time when the glass temperature 0.5 inches in from the periphery has reached its peak value.

Conclusions:

The effect of heater ramp rate and soak time on maximum active element temperature was parametrically investigated for a peak heater temperature of 430 °C. The results indicated that, for realistic thermal processing conditions, maximum allowable active element temperatures were

exceeded when a 1.27 cm (0.5 inch) distance between panel edge and active elements was assumed. However, if a 2.54 cm (1.0 inch) separation distance was allowed, all cases (except the 25 °C/min, 5 minute soak case) showed maximum active element temperatures remaining below 250 °C.

Another way to reduce the maximum active element temperature is to use a lower melting temperature sealing glass. This would allow reduced heater ramp rates which would in turn result in decreased glass panel thermal gradients. Reduced thermal gradients will, of course, reduce glass panel thermal stresses (and glass cracking). Evaluation of lower melting temperature sealing glasses is currently underway.

Copy to:

MS 1435	1800	H. Saxton
MS 0340	1831	F. M. Hosking
MS 1349	1846	W. Hammetter
MS 0549	2476	L. Kovacic
MS 0958	2484	P. G. Stromberg
MS 0841	9100	P. J. Hommert
MS 0828	9102	R. D. Skocypec (route to 9111, 9114, 9115)
MS 0833	9103	J. H. Biffle (route to 9112, 9113, 9116)
MS 0835	9113	T. Bickel
MS 0835	9113	S. E. Gianoulakis
MS 0835	9113	T. E. Voth
MS 0835	9113	Day File
MS 0443	9117	E. L. Hoffman
MS 0443	9117	H. S. Morgan

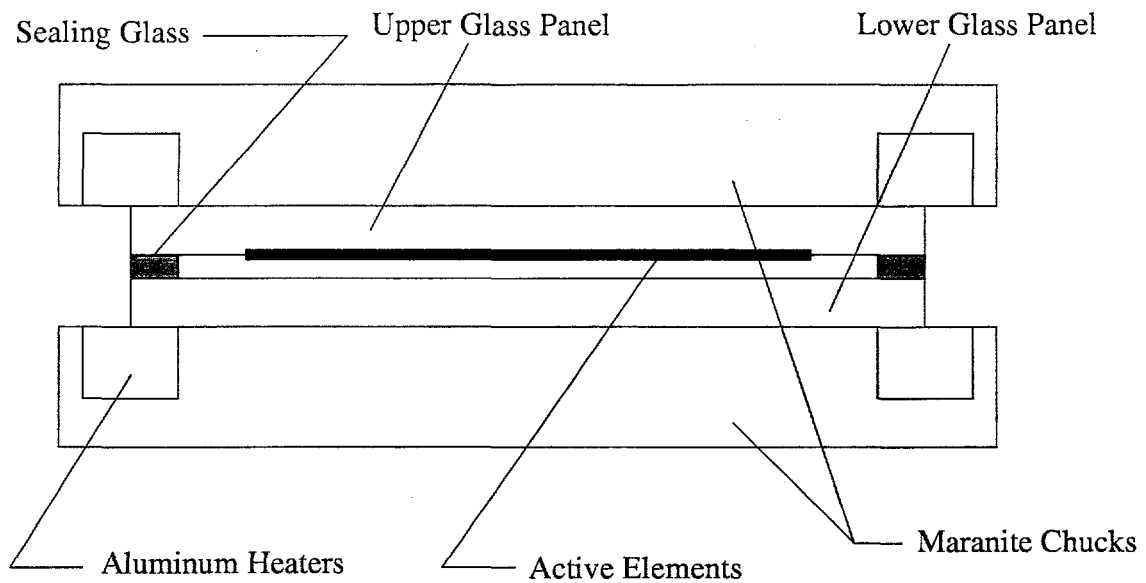


Figure 1 - Schematic of the panel sealing arrangement.

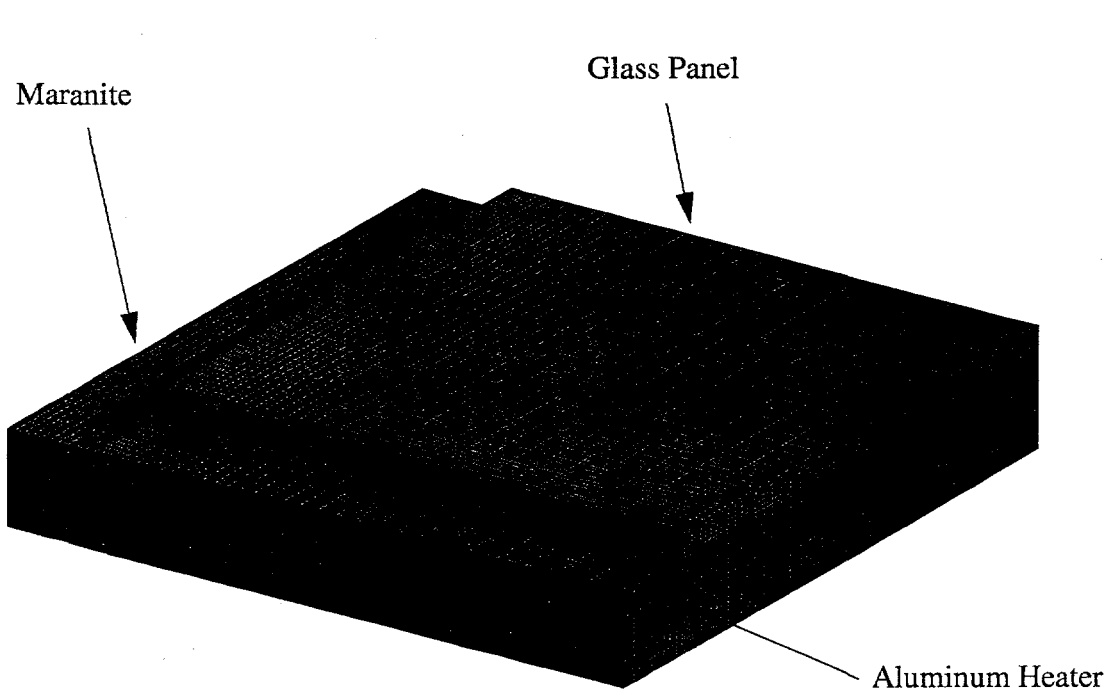


Figure 2 - Finite element mesh employing one-eighth symmetry.

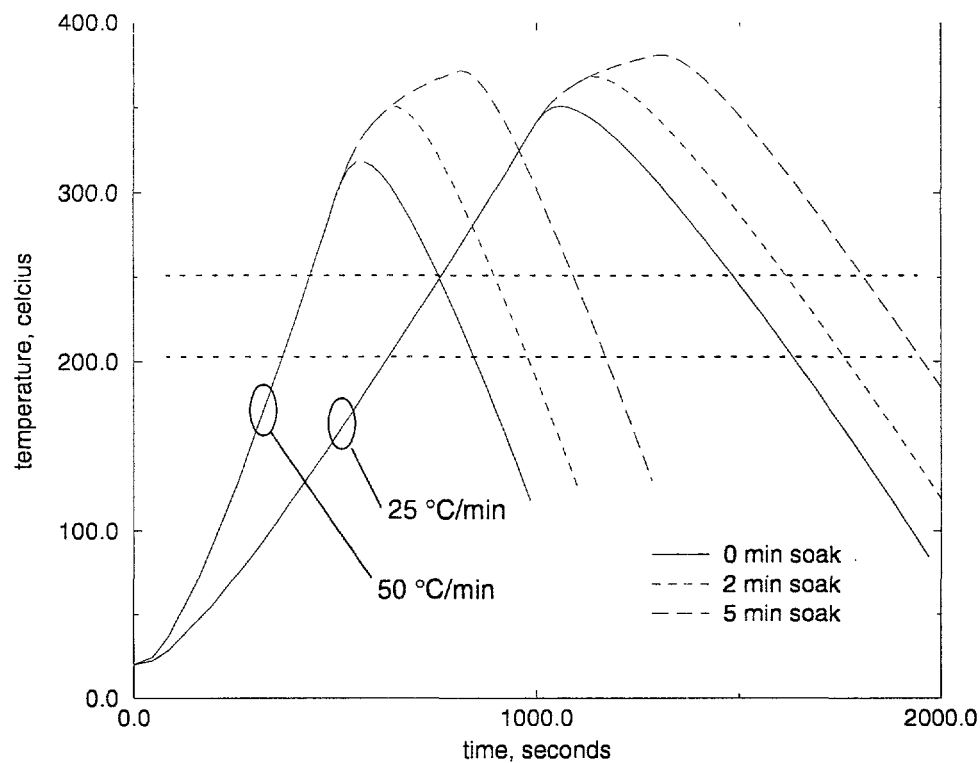


Figure 3 - Active element corner edge temperature histories for a 1.27 cm (0.5 inch) dead-band.

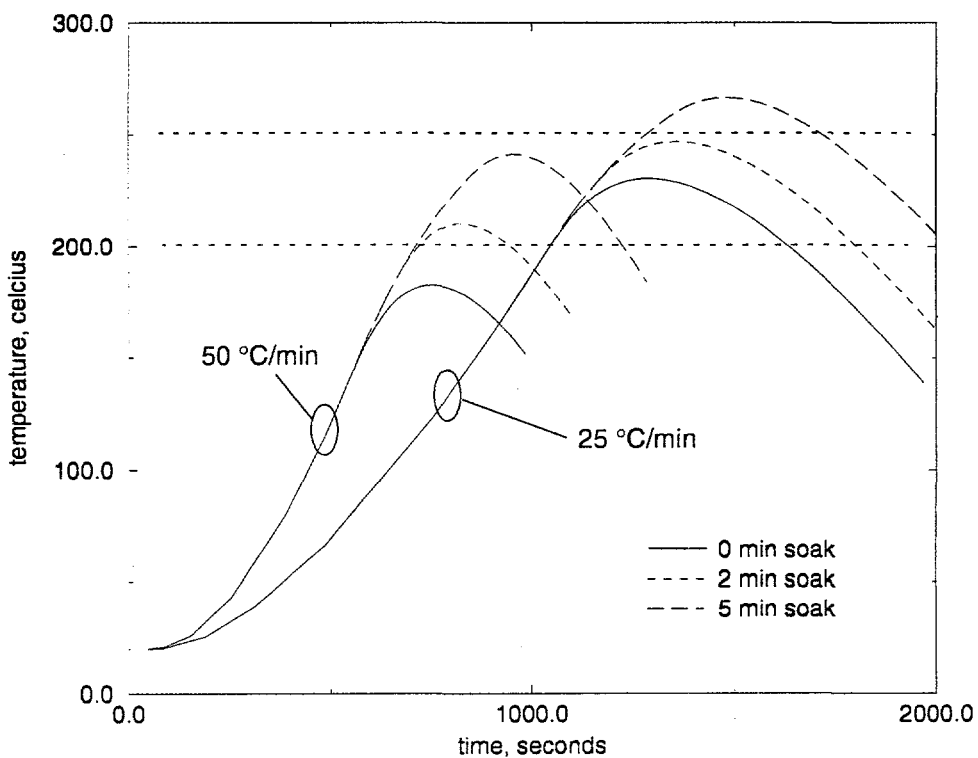


Figure 4 - Active element corner edge temperature histories for a 2.54 cm (1.0 inch) dead-band.

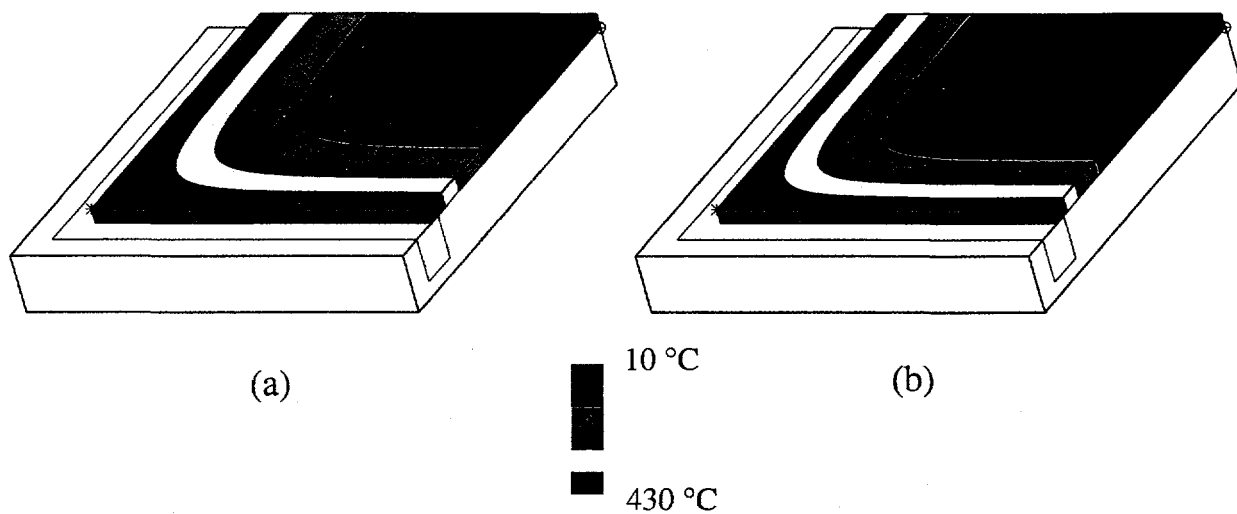


Figure 5 - Temperature contours for the a) 25 °C/min and b) 50 °C/min, 0 minute soak cases at times $t = 1057$ and 551 seconds respectively.

Table 1. Float Glass Temperature-Dependent Material Properties

Property	0 °C	100 °C	300 °C	500 °C	700 °C	900 °C
Thermal Conductivity (W/m•K)	1.34	1.34	1.65	2.14	2.55	
Specific Heat (J/kg•K)	711.76	879.23		1130.4		1236
Density (kg/m ³)	2300.0				2300.0	

Table 2. Maranite Temperature-Dependent Material Properties

Property	0 °C	93 °C	177 °C	205 °C	316 °C	425 °C	600 °C
Thermal Conductivity (W/m•K)	0.13		0.12		0.11	0.12	0.12
Specific Heat (J/kg•K)	1046.6	1046.6		1255.9	1339.7	1423.4	1423.4
Density (kg/m ³)	737.0					737.0	

APPENDIX B

Aug. 28, 1996 memo from J. M. Herlehy, 9113 to S.E. Gianoulakis, Golden Photon Analysis Results.



Sandia National Laboratories

Operated for the U.S. Department of Energy by
Sandia Corporation

date: August 28, 1996

Albuquerque, New Mexico 87185-XXXX

to: Steven E. Gianoulakis, MS 0835, Org. 9113

from: Julie M. Herlehy, MS 0835, Org. 9113

subject: Golden Photon Analysis Results

Problem Background:

Sandia National Laboratories has been examining techniques for sealing glass solar panels using a low temperature frit glass. An active element is screen printed onto the inside surface of the top glass panel. The active element absorbs the sun's energy and converts it into electricity. For reliability purposes, the active element should not exceed 200° C during manufacturing of the solar panel. However, the frit glass, which is in close proximity to the active element, melts at 350° C. Thus a problem is created. If the glass is heated at a fast rate, the heat may not diffuse to the element. Nevertheless, this approach will cause a significant temperature gradient introducing severe thermal stresses in the glass, which may result in cracking. If the glass is heated at a slow rate, the gradient will be minimized, yet, the active element will then most likely exceed its allowable temperature.

A thermal analysis has been performed to evaluate a solar panel sealing process, simultaneous heating of all four edges of the panel. The results of these simulations indicated that the temperature of the active element could not be kept below 200° C while maintaining reasonable thermal stresses in the glass.

This memo will discuss the results of additional simulations where two opposite edges were heated then the remaining two edges were heated. The effort of these additional simulations was aimed at determining whether or not the active element could be kept under 200° C and reasonable thermal stresses in the glass maintained.

Analysis Description:

A series of thermal analyses was performed to evaluate the response of the glass panels to several processing parameters. These parameters included 1) the heating rate, 2) the dwell time defined as the length of time the heater stays at the maximum temperature, and 3) the holding time defined as the length of time between heating one pair of sides and then the other pair. Table 1 lists the ranges of the processing parameters that were evaluated :

Table 1: Parametric Variables

Heating Rate	25° C/min. & 50° C/min.
Dwell Time	0 min., 2 min., & 5 min.
Hold Time	0 Period, 1/2 Period, 1 Period, 2 Periods

Results Description:

Both time-temperature traces and maximum temperatures have been examined. The locations on the glass where the data was taken were 1/2", 1", and 3/2" in from the edge of the glass panel. These locations correspond to the potential edges of the active element. The second viewgraph shows the positions of these data points.

The results from the analyses have been plotted to determine the feasibility of joining the glass panels using a low temperature frit glass. There are two sets of graphs, one set for 25° C/min ramp rate and one set for 50° C/min ramp rate. These graphs show the effects of different hold times for 0, 2, and 5 minute dwell times. When 0 period hold time was graphed, the data was extracted from 0.5" in from the corner because it had the highest peak temperature when both heaters were simultaneously active. For the staggered heating, the data was extracted from 0.5" in from the left edge. It had the highest peak temperature because it was preheated by the first heater before it was heated by the second heater.

Conclusion:

There is a reduction in peak (maximum) temperatures when the heaters are staggered, as seen in the third through the eighth viewgraph.. However, there is no improvement in increasing the time between firing the second heater after the first heater. This indicates that there is no advantage of using a hold time greater the 0.5 period. All it would do is increase the production time. The ninth viewgraph shows the differences between hold times from 25° C/min ramp rate and for 50° C/min ramp rate.

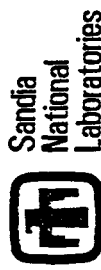
By comparing a fixed dwell time and a fixed hold time, it has been observed that using a higher ramp rate results in a lower peak temperature. When comparing a fixed ramp rate and a fixed hold time, it can be seen that using a longer dwell time results in a higher peak temperature.

Copy to:

MS 0835 9113 T.E. Voth
 MS 0835 9113 T.E. Bickel

Golden Photon Parametric Variables

Engineering Sciences Center



The following process parameters have been examined to determine their effect on the active element thermal response.

Heating Rate	25° C/min. & 50° C/min.
Dwell Time	0 min., 2 min., 5 min.
Hold Time	0, .5P, P, 2P

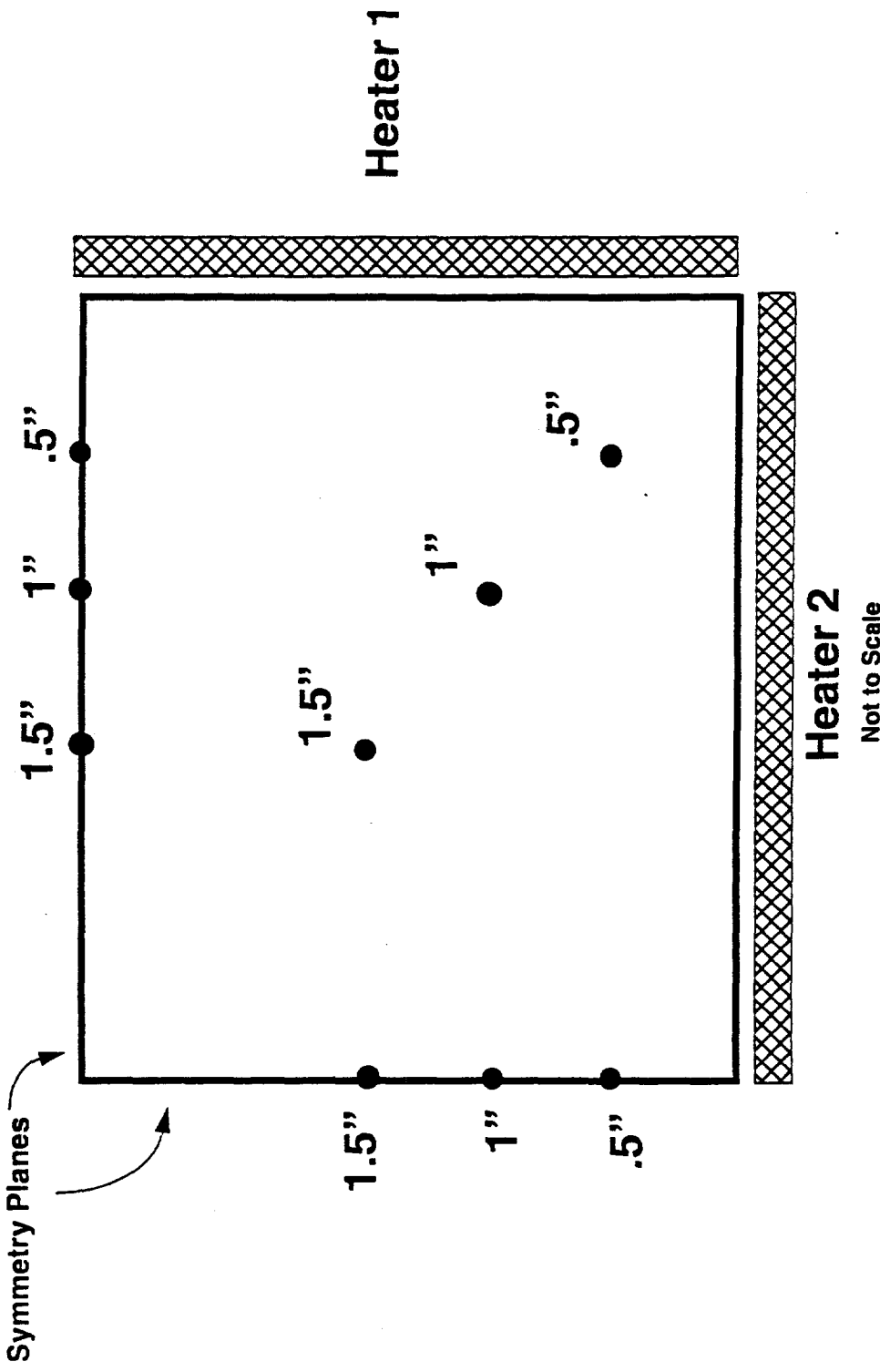
Golden Photon Data Points

Engineering Sciences Center



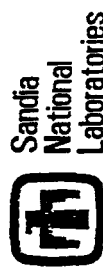
Sandia
National
Labs

Quarter Symmetry Region of Panel

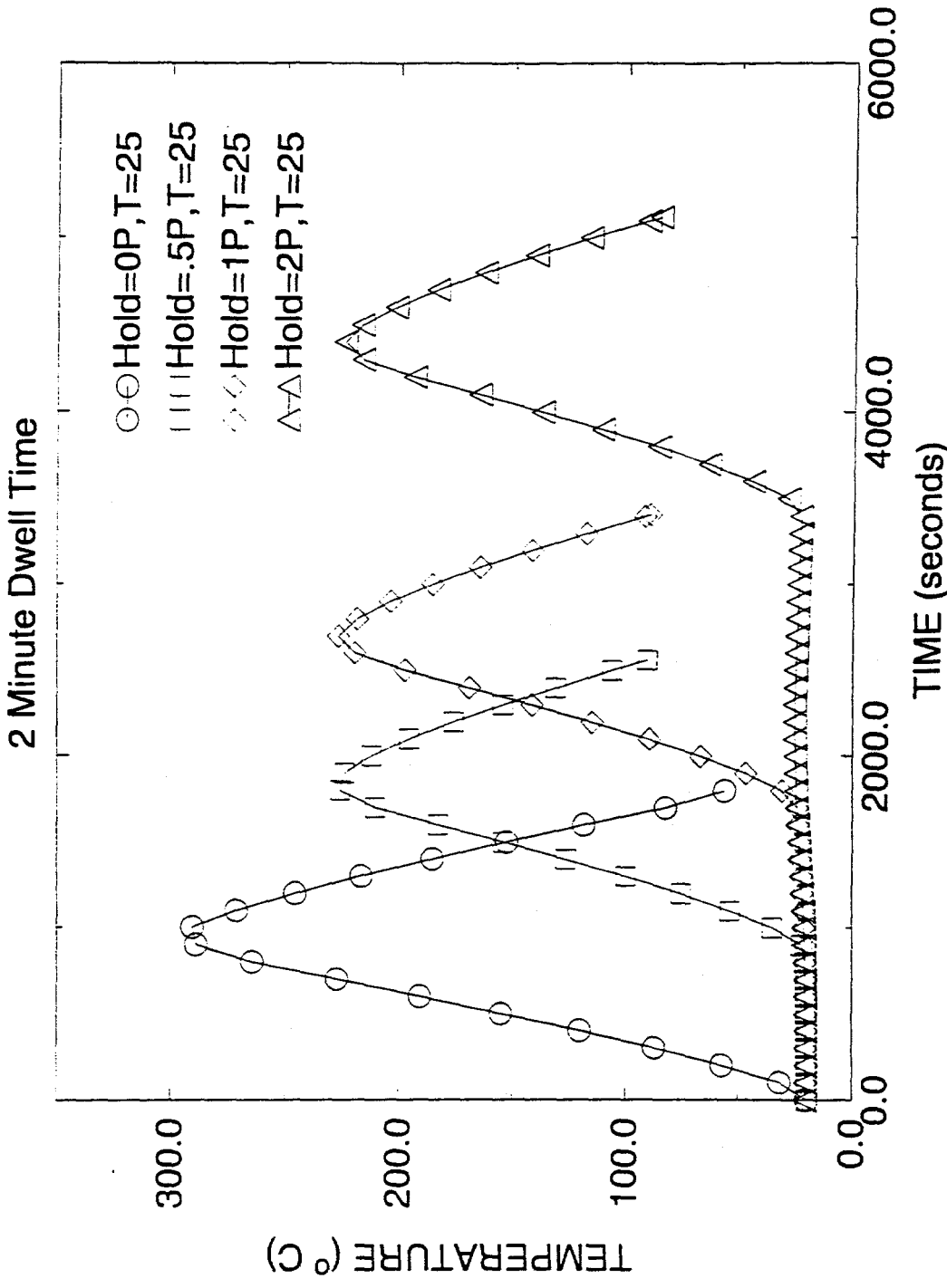


Golden Photon Hot Spot Temperature Predictions

Engineering Sciences Center



Difference in Hold Times

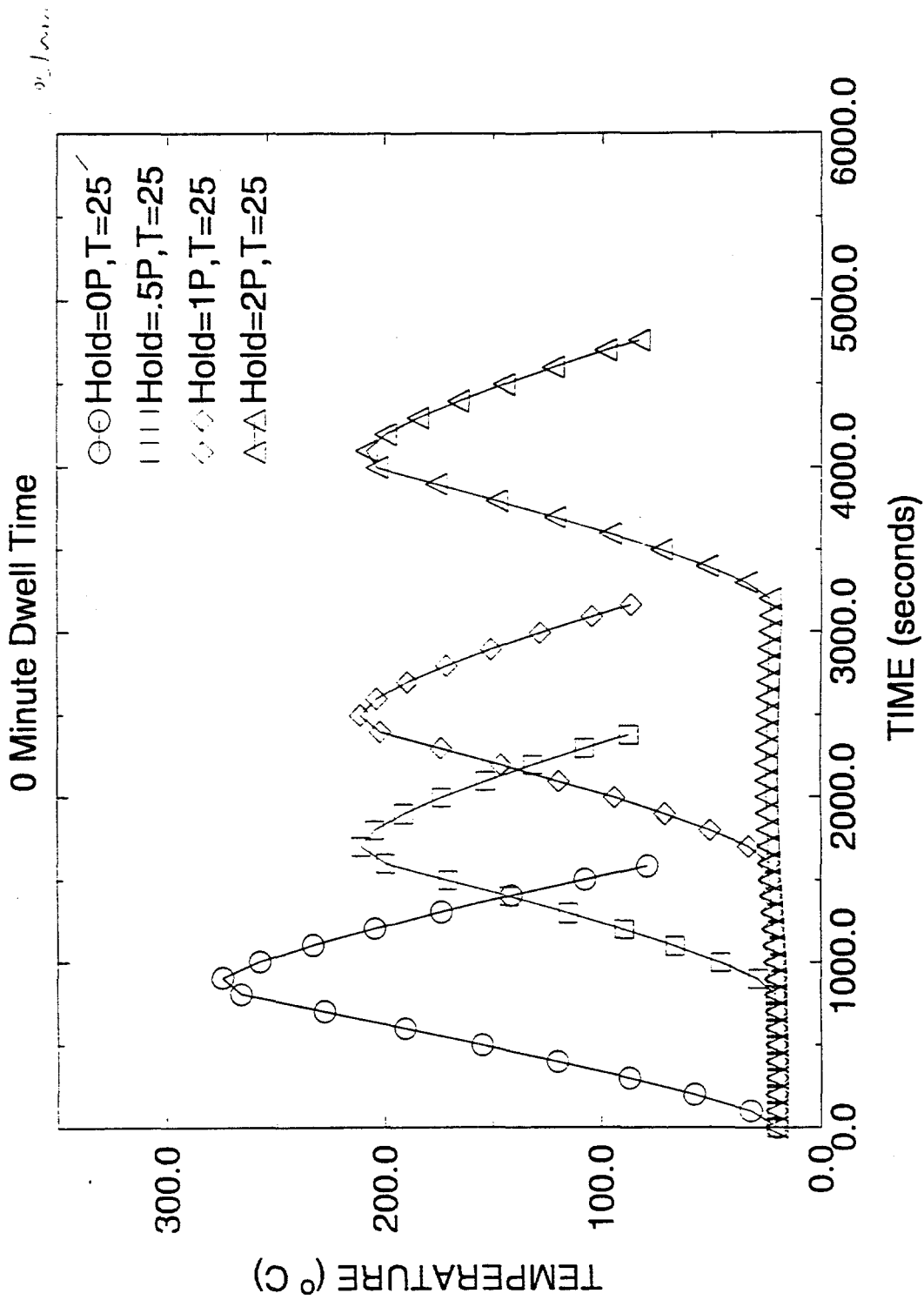


Golden Photon Hot Spot Temperature Predictions

Engineering Sciences Center

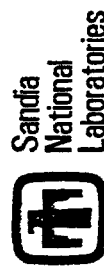


Difference in Hold Times

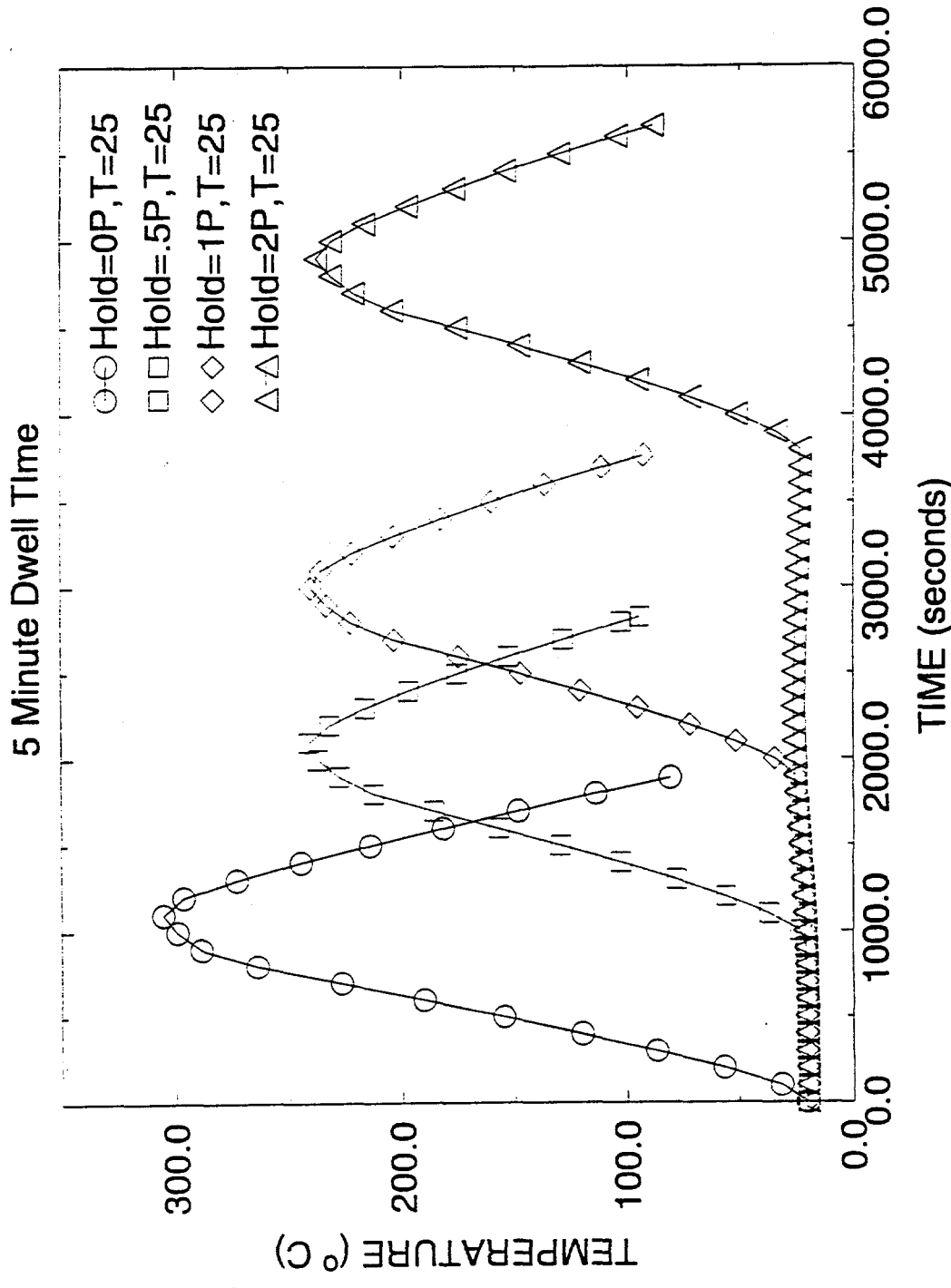


Golden Photon Hot Spot Temperature Predictions

Engineering Sciences Center



Difference in Hold Times



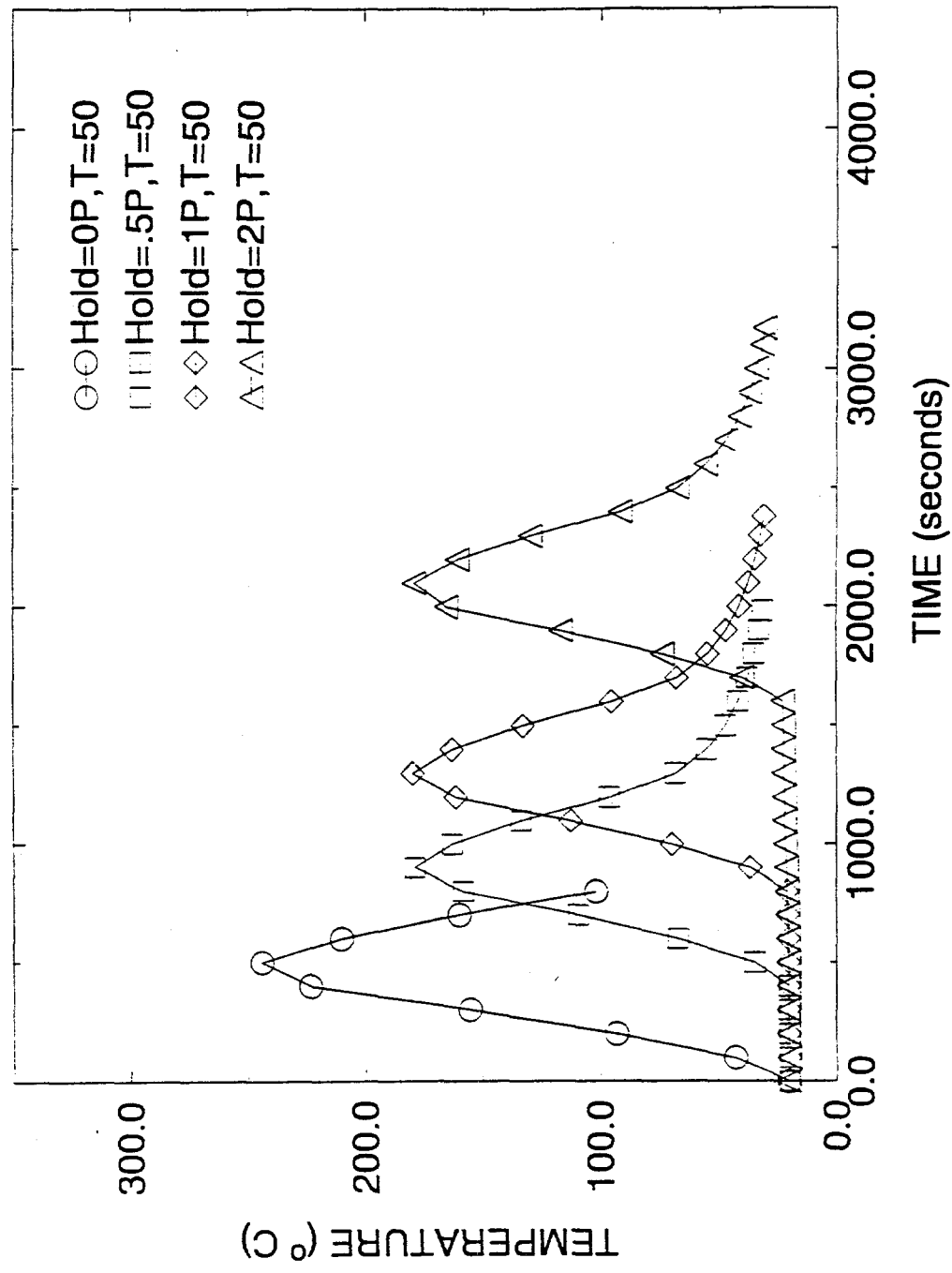
Golden Photon Hot Spot Temperature Prediction

Engineering Sciences Center



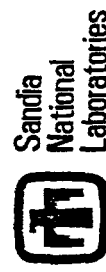
Difference in Hold Times

0 Minute Dwell Time



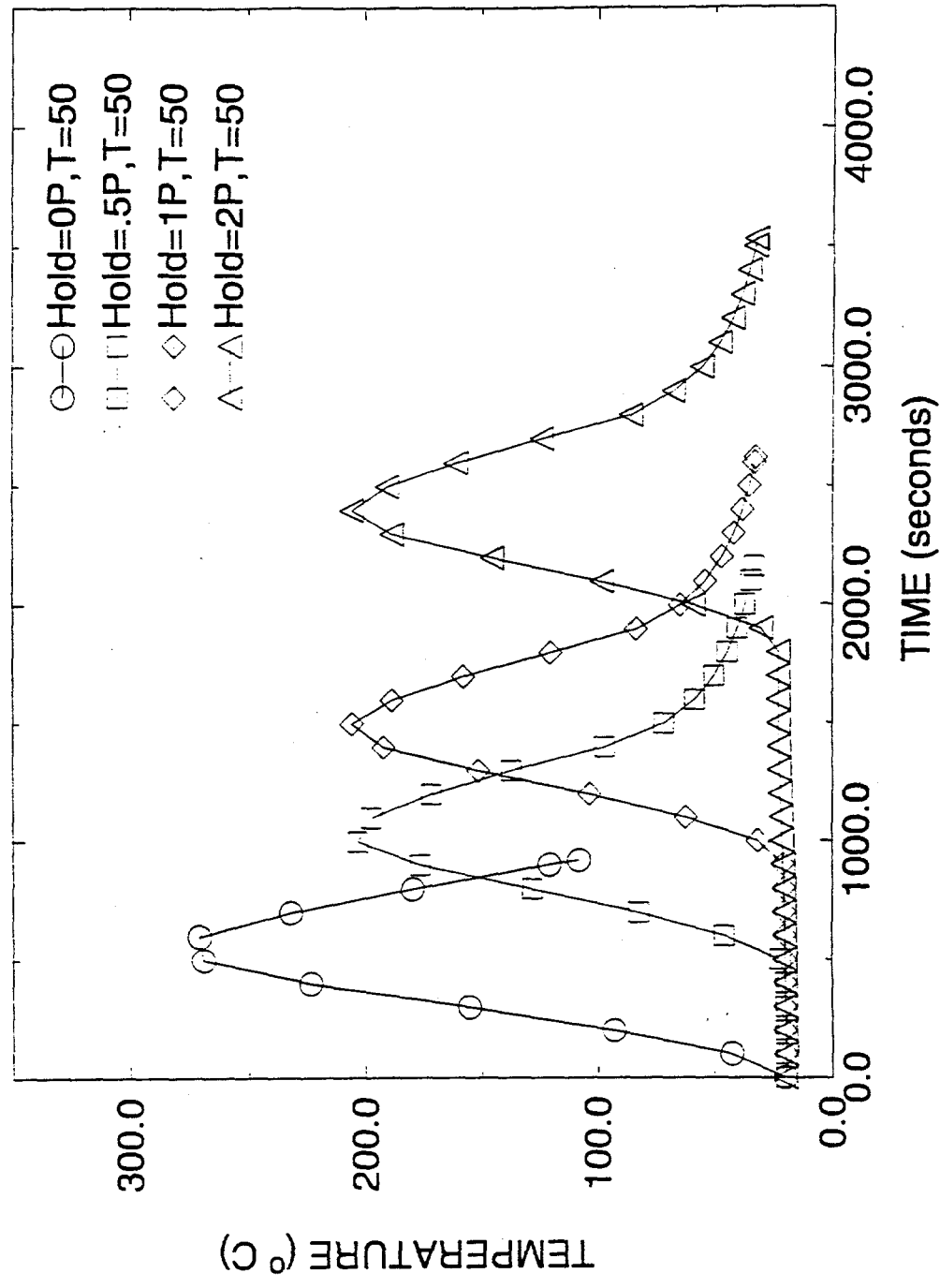
Golden Photon Hot Spot Temperature Predictions

Engineering Sciences Center



Difference in Hold Times

2 Minute Dwell Time

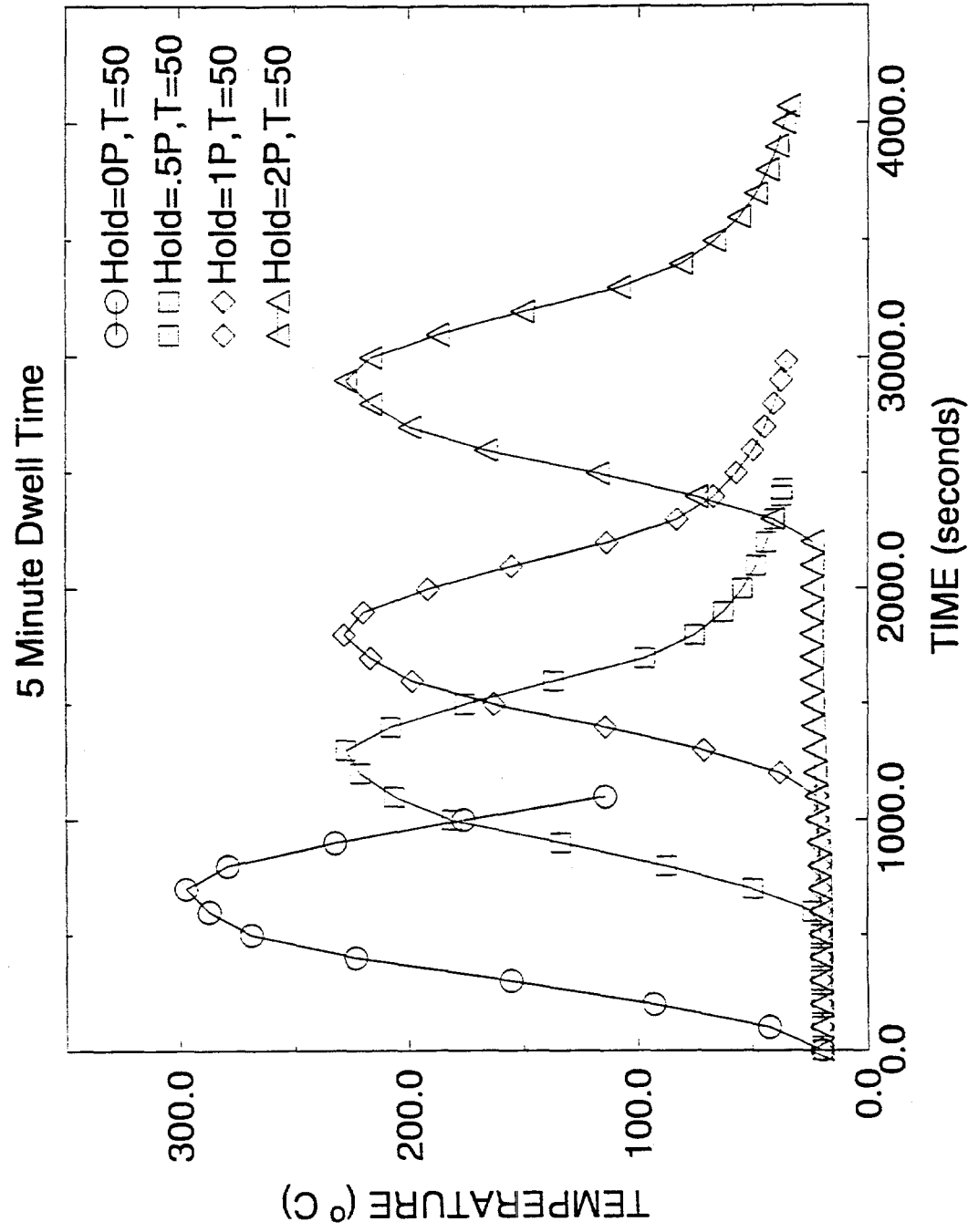


Golden Photon Hot Spot Temperature Predictions

Engineering Sciences Center

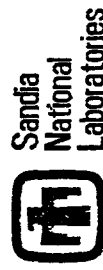


Difference in Hold Times



Golden Photon Peak Temperatures

Engineering Sciences Center



Peak Temperatures Exhibited by Active Element

Dwell Time	25° C/min, 0 Hold	25° C/min, .5P Hold	50° C/min, 0 Hold	50° C/min, .5P Hold
0 minutes	274° C	211° C	244° C	163° C
2 minutes	290° C	223° C	271° C	203° C
5 minutes	306° C	241° C	297° C	227° C

APPENDIX C

July 22, 1996 memo from E. L. Hoffman to S. J. Glass, 1845, Structural Analysis of a Solar Panel Sealing Process.

date: July 22, 1996

to: S. J. Glass, 1845

from: Edward L. Hoffman

subject: Structural Analysis of a Solar Panel Sealing Process

1 Introduction

This report presents the structural considerations of a process proposed for hermetically sealing two 609.6 mm-square (24 inch-square) glass panels while maintaining temperatures 12.7 mm (0.5 inches) inward from the edge of the panels below 250 °C. The reason for the temperature constraint is that one of the glass panels contains active solar elements which are deposited over the surface, starting 12.7 mm from the edge of the panel, in an earlier process. If heated above 250 °C, these active elements will degrade. The region of glass without active element coating is known as the "dead-zone." In the proposed process, a strip of sealing glass is sandwiched in the dead-zone between two glass panels. The panels are then heated around the periphery to melt the sealing glass, creating a hermetic seal. The proposed sealing glass (Plasmaco frit) has a melting temperature of 430 °C, which is substantially lower than the melting temperature of the glass panels (float glass). The challenge of the proposed process is to heat the periphery of the glass panels to 430 °C and then cool it before the active element region can reach 250 °C. Initially, 152.4 mm-square (6 inch-square) mock-ups of the solar panel will be manufactured to determine the feasibility of this process and test the hermeticity of the joints. Only the length and width of the glass panels are scaled. The glass thickness, spacing and dead-zone width will be the same as the full-size unit. A thermal analysis was performed to determine the heating rates and hold times required to achieve the process goal [1]. Results of the thermal study indicated that, for realistic heating rates, peak active element temperatures exceeded 250 °C. The thermal study concluded that the process goal could be achieved if the dead-zone were widened to 25.4 mm (1 inch). Even if the dead-zone is widened and the thermal requirements are met, the high thermal gradients resulting from this operation will cause differential thermal expansion of the glass panels, producing stresses in the float glass. This memo presents structural simulations of the sealing process which were performed to determine if the proposed thermal process will produce stresses in the glass panels which are greater than the tensile strength of float glass. Simulations were also performed to determine if the 152.4 mm mock-up accurately represents the mechanical and thermal response of a full-size unit. The structural calculations were performed using JAC3D [2], utilizing the results of the thermal studies as input into the structural calculations.

2 Model Description

The structural calculations presented in this memo consider only the glass panels which are sealed together. Because the sealing glass is not considered in these calculations, the development of residual stresses due to the differential thermal expansion between the glass panels and the sealing glass is not simulated. Such residual stresses are expected to be much smaller than the in-process stresses. For this reason, simulations of residual stress formation will not be performed until manufacturability is proven.

The finite element model of the proposed glass panel sealing apparatus is shown in Figure 1. The model shown is of a 152.4 mm-square glass panel which is 3.175 mm-thick. Utilizing the three symmetry planes in the geometry, a one-eighth symmetry model was developed. The entire glass/frit assembly is sandwiched between two heater chucks consisting of an aluminum heating element and a Marinite insulating block. Though necessary for the thermal simulations [1], the heating chuck was not required for the structural simulations but is shown in Figure 1 to demonstrate the symmetry of the thermal boundary conditions. Hence, the structural model consists only of a quarter of one of the glass panels.

The float glass mechanical properties are assumed to be temperature-independent, with an elastic modulus $E = 70$ GPa, Poisson's ratio $\nu = 0.23$, and thermal expansion coefficient $\alpha = 94.0 \times 10^{-7} \text{ }^{\circ}\text{C}^{-1}$. Symmetry boundary conditions were applied along the two through-thickness planes of the glass. Symmetry boundary conditions were not placed on the third symmetry plane as the two glass panels are separated by a small gap. The results of the thermal simulations were entered as input into the structural simulations. Although the thermal analyses investigated many heating rate and hold time combinations, the only combination used in the structural simulation was the one which yielded the most favorable

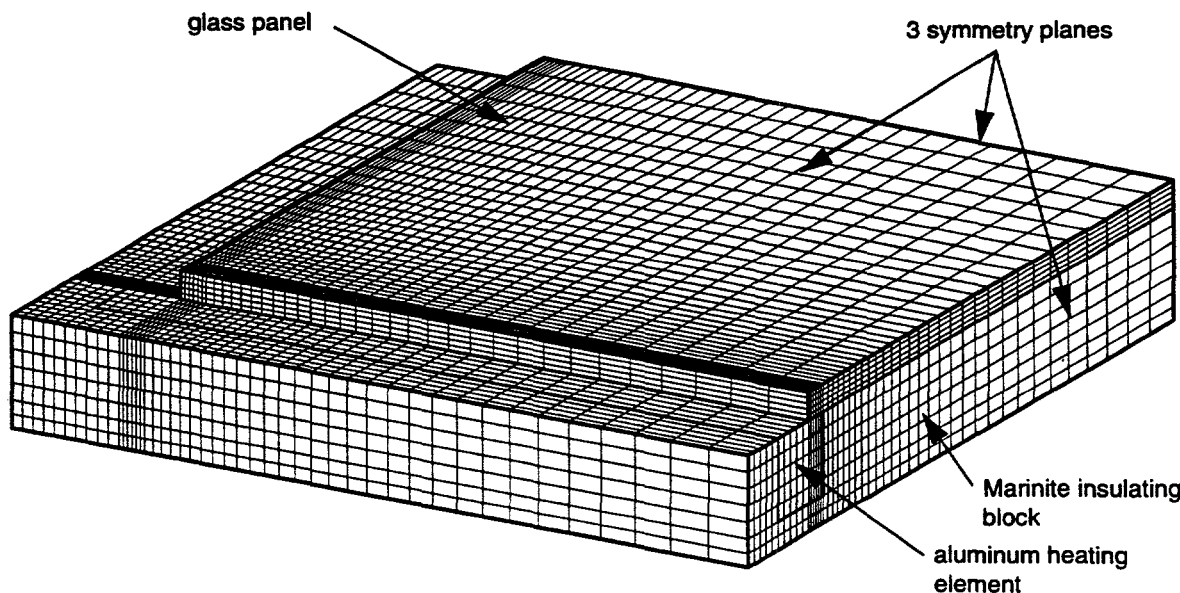


Figure 1. Finite element model of the 152.4 mm-square glass panel. The aluminum heating element and Marinite insulating block are not included in the structural simulations.

thermal results, a 50 °C/min heating rate with a 0 min hold time. To heat from room temperature (20 °C) to 430 °C and then back to room temperature at a rate of 50 °C/min requires 984 seconds to complete.

3 Analysis Results

The structural performance of the glass panels is presented in terms of the maximum principal stress, as maximum principal stress controls fracture in low fracture toughness materials such as float glass. Although the maximum temperature is attained at 492 seconds, the maximum thermal gradient occurs at a later time. Figure 2 is a plot of the temperature and maximum principal stress distribution in the 152.4 mm glass panel at 571 seconds, the time at which the largest maximum principal stress occurs. The maximum temperature occurs at the corner of the panels. However, the maximum principal stress of 39.8 MPa occurs inside of the corner.

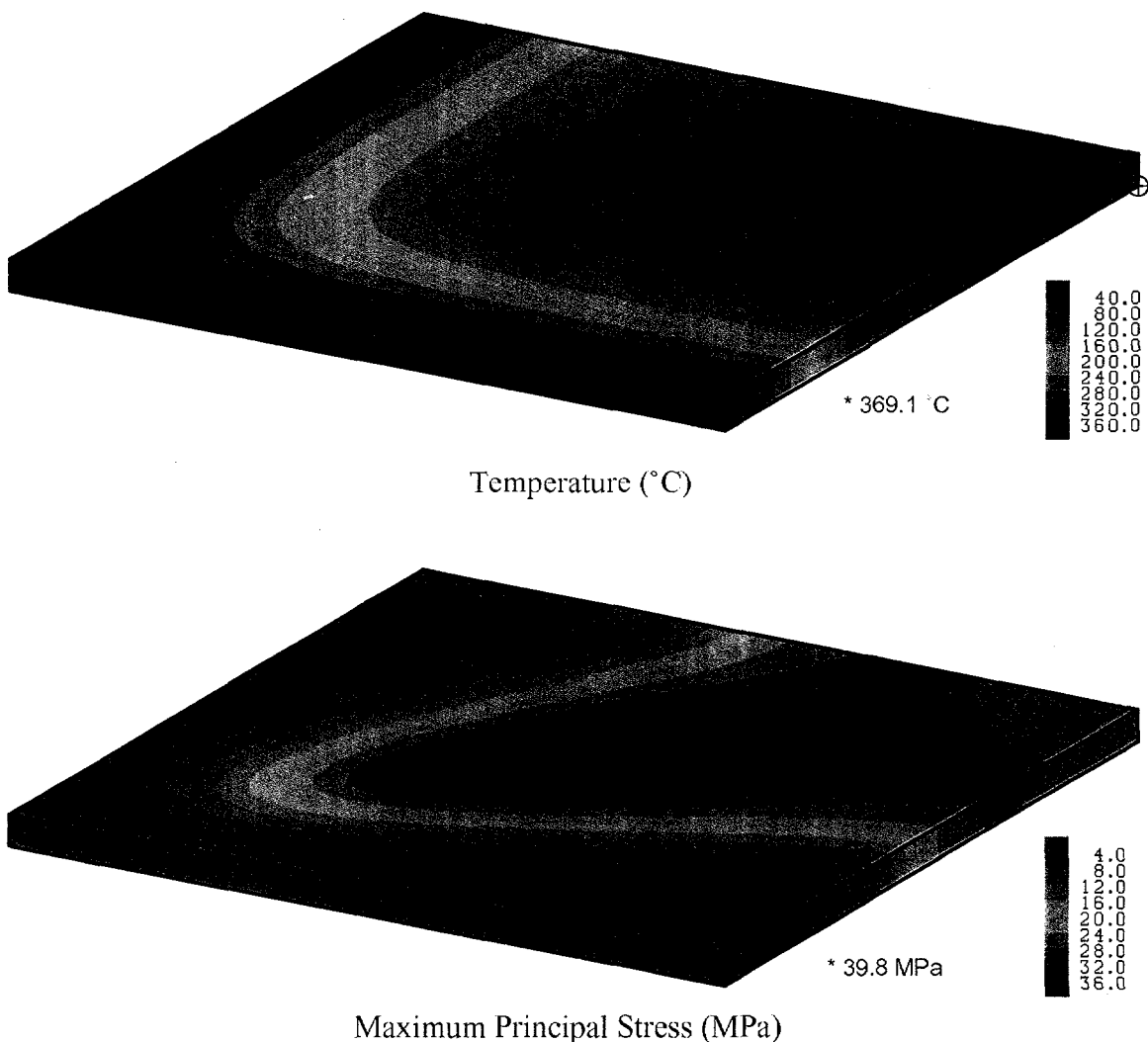


Figure 2. Temperature and maximum principal stress distribution in the 152.4-mm glass panel at 571 seconds, the time at which the largest maximum principal stress occurs.

Allowing for a safety factor, the allowable design stress for annealed soda-lime glass under sustained loading for 1000 hours or more is 7 MPa. Glass exhibits a time-load effect. Hence, a glass article breaks at a lower stress under prolonged loading than under momentary loading. In practice, glass products with surface imperfections will exhibit a short-term strength of nearly 70 MPa. Since the duration of the peak stresses due to the proposed sealing operation are relatively short (~ 1 min), the glass panels may be capable of withstanding this momentary extreme. However, since the factor of safety is small, the probability of fracture will be highly dependent on the condition (i.e. surface condition, flaw distribution, etc.) of the glass panels. The fact that the peak stress is not located near the cut edges of the glass will reduce the likelihood of failure.

Because the cool region of glass would be proportionately larger in a full-size solar panel than in the 152.4 mm test specimen, concern was raised as to whether the 152.4 mm solar panel accurately represented the thermal and mechanical response of the full-size unit. Since the maximum stress occurred toward the center of the 152.4 mm unit, the maximum stress might actually be smaller in a full-size unit because there would be a larger cool region to strain. Hence, the same thermal and structural calculations were repeated for a full-size 609.6-mm-square solar panel. All of the same assumptions and boundary conditions were applied to this model. Figure 3 is a plot of the temperature and maximum principal stress distribution in the 609.6-mm glass panel at 571 seconds. Like the 152.4 mm unit simulation, this is the time at which the largest maximum principal stress occurs. Local to the edges, the thermal response appears to be the same as that predicted for the quarter-symmetry model, exhibiting the same maximum temperature and temperature gradient. As expected, the larger cool region of glass results in smaller stresses in the center of the plate. However, the maximum stresses in the full-size unit are exactly the same as those predicted for the 152.4 mm panel. Hence, the magnitude of the maximum stress is due to the temperature distribution at the corner of the glass panel. The glass is trying to expand uniformly along the outside edges but is constrained from doing so by the cooler inner region of glass. On the sides of the panel, the expanding glass is constrained in one direction (parallel to the edge). However, at the corner of the panel, the expanding glass is constrained in two directions. The close comparison between the full-size and 152.4 mm units is due to the fact that the temperature gradients in the corner of the glass are exactly the same for these two models. Hence, for the proposed heating concept, the 152.4 mm mock-ups assembled for proof of concept accurately represent the mechanical and thermal response of a full-size unit.

4 Conclusions

Finite element simulations of a proposed glass sealing process were performed to: (1) determine the mechanical response of 152.4 mm solar panels manufactured for proof-of-concept, and (2) determine if the 152.4 mm mock-up accurately represents the mechanical and thermal response of a full-size unit. The simulations yielded nearly identical thermal and mechanical results for both the full-size unit and the 152.4 mm mock-up, indicating that the 152.4 mm mock-ups accurately represent the mechanical and thermal response of a full-size unit. The simulations revealed that the magnitude of the largest maximum principal stress is the result of the large temperature gradient at the corners of the glass panel. In the corners of the panels the expanding glass is constrained in two directions. The large temperature gradient

in the corners (a product of the rapid heating rate) resulted in a predicted maximum stress of over 39 MPa, much larger than the 7 MPa design stress usually used for float glass. However, since the duration of the peak stresses due to the proposed sealing operation are relatively short (~ 1 min), the glass panels may be capable of withstanding this momentary extreme. These large stresses could be reduced by reducing the heating/cooling rate. However, this would undoubtedly result in a thermal response which would not satisfy the process requirements of maintaining temperatures below 250 °C in the active-element region. Another way to circumvent the high thermally-induced stresses inherent to this process is to sequentially heat the parallel edges of the panel. This modification to the sealing process would eliminate the high temperature gradients in the corners of the glass which produce the large stresses. This modification to the sealing process will be investigated next.

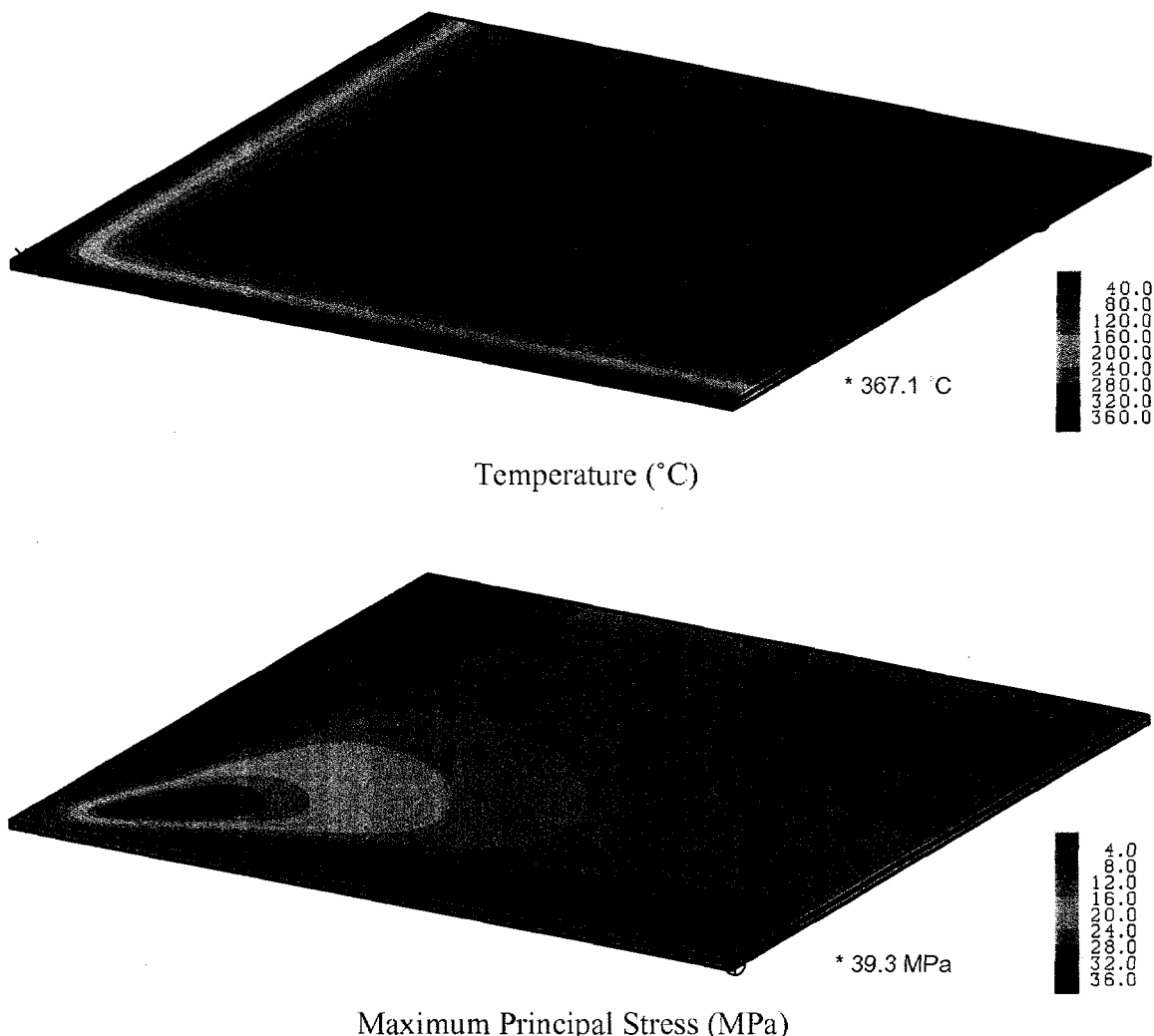


Figure 3. Temperature and maximum principal stress distribution in the 609.6-mm glass panel at 571 seconds, the time at which the largest maximum principal stress occurs.

5 References

- 1 S. E. Gianoulakis and T. E. Voth, "Thermal Analysis of a Solar Panel Sealing Process for the Golden Photon CRADA," internal memorandum to S. J. Glass, Sandia National Laboratories, Albuquerque, New Mexico, May 17, 1996.
- 2 J. H. Biffle, "JAC3D - A Three-Dimensional Finite Element Computer Program for the Nonlinear Quasi-Static Response of Solids with the Conjugate Gradient Method," SAND87-1305, Sandia National Laboratories, Albuquerque, New Mexico, February, 1993.
- 3 D. C. Boyd, D. A. Thompson, *Kirk-Othmer: Encyclopedia of Chemical Technology*, pp. 807-880, John Wiley & Sons, Inc., 1980.

Distribution

MS0958	1484	P. Stromberg
MS0549	1492	L. Kovacic
MS1411	1831	F. M. Hosking
MS1134	1833	B. Damkroger
MS1349	1846	J. Bullington
MS1349	1846	W. F. Hammetter
MS0841	9100	P. J. Hommert
MS0835	9102	R. D. Skocypec (Route to 9111)
MS0833	9103	J. H. Biffle (Route to 9116)
MS0828	9104	E. D. Gorham (Route to 9114, 9115)
MS0834	9112	A. C. Ratzel (Route to 9113)
MS0835	9113	S. Gianoulakis
MS0835	9113	T. Voth
MS0443	9117	R. S. Chambers
MS0443	9117	E. L. Hoffman
MS0443	9117	H. S. Morgan (Route to 9117)
MS0443	9117	S. N. Burchett
MS0443	9117	QA File
MS0437	9118	E. P. Chen (Acting) (Route to 9118)
MS0439	9234	D. R. Martinez

APPENDIX D

Sept. 24, 1996 memo from P. M. Baca, 1833 to S. J. Glass, 1833.

Sandia National Laboratories

Albuquerque, New Mexico 87185-0367

date: September 24, 1996

to: S. Jill Glass, MS-0367, Dept. 1833

from: Paul M. Baca, MS-0367 (1833)
845-7133

We originally met in your office on 8/14/96 to discuss options in sealing the Golden Photon photovoltaic collector. You showed me a test unit, and explained that two other sealing methods were being researched here at Sandia. I have read correspondence between Golden Photon and Sandia, have spoke to Scot Albright at GP, and have contacted Various GP suppliers.

Performance goals include:

- 100 times less water absorption
- Materials compatibility with; soda lime glass, aluminum, various PV surfaces, (Ni-Cr, SnO₂, Cu, Cr-Pd-Au, etc.)
- Possible elimination of an edge seal
- Elimination of a desiccant
- Ease of assembly
- A 15 to 20 year life span
- An 85 degree F, 85% RH operational environment

Scot says that the collector has undergone several iterations since he gave you the part that you have in your office. As of July 1996, the stainless steel spacer will be removed, a "U" shaped edge band will replace the aluminum extrusion, and a different desiccation system will be added. Formerly, they used HB Fuller TL-0471 urethane as an edge sealant. The new spacerless design will use Fuller's UR-5127H urethane.

GP's surface preparation and assembly follows these guidelines:

- Glass panes are cleaned with Alconox, water rinsed, and towel dried
- An edge margin about 0.35" is ground around the periphery of one pane using a 220 grit diamond wheel
- ADCO's PIB-7, (polyisobutylene), which contains 0.010" diameter glass beads is applied to one glass surface
- The panes are matched together and bonded
- A urethane adhesive is applied to the periphery of the panes and the retention channel, ("U" shaped band), is applied

In order to reach the level of performance that GP expects, surface preparation prior to bonding becomes a major consideration. I suggest the following:

- Perform all work in a clean environment
- Wear powder free butyl rubber gloves and a dust mask
- Degrease the glass with MEK or acetone
- Mask and abrade both surfaces to be sealed with 600 grit abrasive
- Unmask and wash all surfaces with 1 tbs. Alconox to one gallon water
- Rinse with DI water
- Dry in oven at 200 degrees F
- While warm, etch each edge with a solution of chromium trioxide, (1 pbw), to DI water, (4 pbw), for 10 minutes
- Rinse off the immersed edge with DI water and immerse the next edge, rinse and repeat until all edges have been etched and rinsed
- Oven dry the glass at 100 degrees F
- Allow the glass to cool
- Degrease edges with MEK or acetone
- Blow dry with clean compressed air
- Apply sealant and cure

I realize that this procedure is more extensive than what is currently used. I am concerned that GP is not getting better permeability figures for this material. Several reasons may account for this. Most importantly, the current surface preparation in conjunction with the glass beads may be creating leakage paths at the interface of the ground glass and the glass beads.

Grinding glass correctly is not a trivial operation. In order to avoid imparting unwanted physical anomalies to the glass, the wheel must be dressed properly. The wheel must then be fed incrementally to the glass, and traverse smoothly across the glass while the work remains rigidly fixtured. A liquid coolant should be used to remove fines and avoid over heating.

I suggest a finer abrasive. A 220 grit diamond wheel has an average micron size of 66. By going to a 600 grit aluminum oxide paper, size drops to about 15 microns. This reduction in groove depth will minimize leakage paths while offering mechanical interlock.

PIB is one of the best materials available for this type application. I calculate that on a 24" square panel utilizing a 0.010" bondline, there would be 0.96 square inches of exposed adhesive. Water accumulation figures given to me by GP on units incorporating a spacer and desiccant, suggest the permeability for this system exceeds the value normal for this material. However, PIB formulations vary widely from manufacturer to manufacturer as do their properties.

ADCO will not reveal the glass bead loading on their PIB-7 material as it was originally produced for another consumer and its nature is proprietary. It may be that the loading is too high for this application. They also will not say whether or not the beads have been treated with a coupling agent. This is critical to the bead/sealant interface. I would like to see testing done with PIB-3, which has no beads.

Other materials should be considered. There are butyl compounds that can match PIB's moisture permeability and may offer better wet-out and adhesion to the glass. Polyvinyl butyral is used extensively in glazing applications. Also, there are urethanes on the market which initially have higher moisture permeability, but then couple with water molecules after a time. This coupling retards further permeation unless the differential pressure of the water vapor becomes significant.

The concept of differential pressure is noteworthy. GP currently uses a beaded desiccant between the panes to capture water. In the future, they plan to remotely locate a desiccant canister that will also relieve the ratcheting that takes place during expansion and contraction of the panes. In effect, they have built a pump with a semi-permeable membrane. An alternative may be to seal the glass, but locate the desiccant source between the seal, and the "U" channel. This would require a fillet on either side of the channel against the glass. The desiccant could then be plumbed to the space between the aluminum channel and the glass.

Instead of a desiccant, an internal pressure source such as a compressed gas with a molecular orifice, or a sublimation material may provide positive internal pressure.

I would like the opportunity to visit and exchange ideas with GP. Much could be learned from a hands on tour. Please contact me if you plan a visit in the near future.

Copy to:
BK Damkroger, MS-0367, Dept. 1833

APPENDIX E

Hardware Drawings.

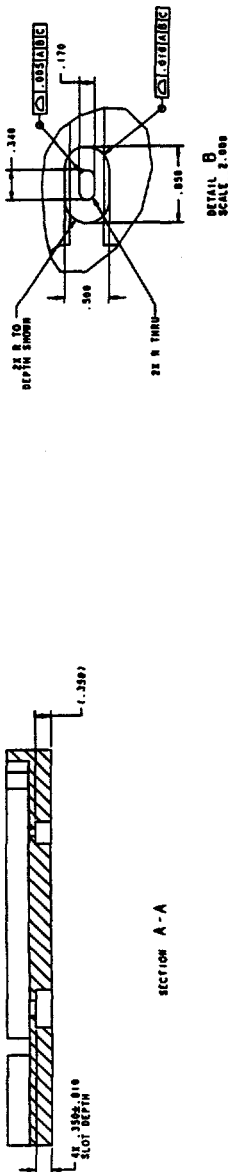
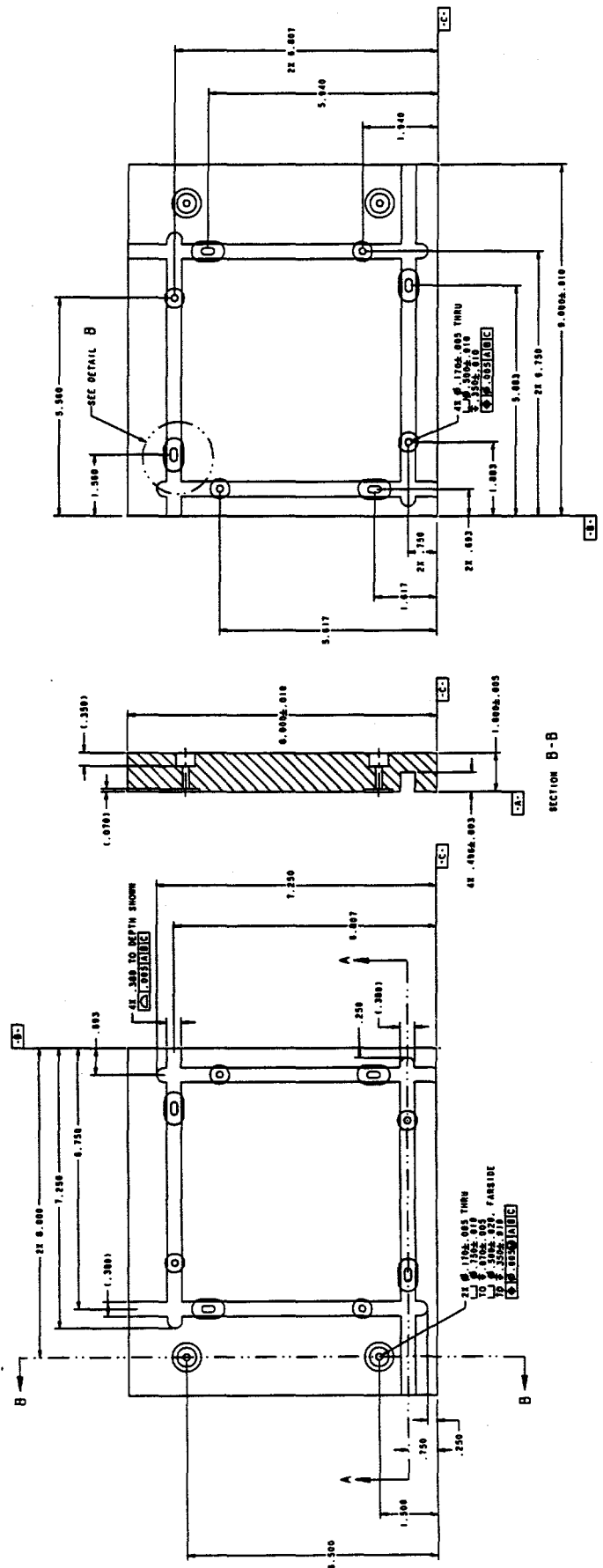
UNCLASSIFIED

NOTES:

- GENERAL REQUIREMENTS PER SPECIFICATION.
- MATERIAL: MARSHALITE, 1.00 INCH.

NAME AND NUMBER		REF.	REVISION	REVISION	DATE	NAME	NAME
531427-000	A	1	1	1	1	1	1

Page 1



NOTE	PLATE (TOP)				
	1	2	3	4	5
NAME	A				
TYPE CLASSIFICATION	UNCLASSIFIED	E	UNCLASSIFIED	E	UNCLASSIFIED
NAME CLASSIFICATION	UNCLASSIFIED	E	UNCLASSIFIED	E	UNCLASSIFIED
NAME	531427-000	531427-000	531427-000	531427-000	531427-000
DATE	10-10-1988	10-10-1988	10-10-1988	10-10-1988	10-10-1988
UNCLASSIFIED	1	2	3	4	5

PLATE (BOTTOM)					
NAME	531427-000	531427-000	531427-000	531427-000	531427-000
TYPE CLASSIFICATION	UNCLASSIFIED	E	UNCLASSIFIED	E	UNCLASSIFIED
NAME CLASSIFICATION	UNCLASSIFIED	E	UNCLASSIFIED	E	UNCLASSIFIED
NAME	531427-000	531427-000	531427-000	531427-000	531427-000
DATE	10-10-1988	10-10-1988	10-10-1988	10-10-1988	10-10-1988
UNCLASSIFIED	1	2	3	4	5

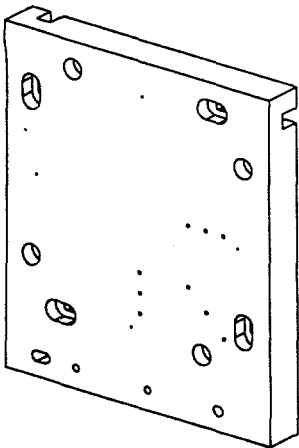
PLATE (TOP)					
NAME	A				
TYPE CLASSIFICATION	UNCLASSIFIED	E	UNCLASSIFIED	E	UNCLASSIFIED
NAME CLASSIFICATION	UNCLASSIFIED	E	UNCLASSIFIED	E	UNCLASSIFIED
NAME	531427-000	531427-000	531427-000	531427-000	531427-000
DATE	10-10-1988	10-10-1988	10-10-1988	10-10-1988	10-10-1988
UNCLASSIFIED	1	2	3	4	5

PLATE (TOP)					
NAME	A				
TYPE CLASSIFICATION	UNCLASSIFIED	E	UNCLASSIFIED	E	UNCLASSIFIED
NAME CLASSIFICATION	UNCLASSIFIED	E	UNCLASSIFIED	E	UNCLASSIFIED
NAME	531427-000	531427-000	531427-000	531427-000	531427-000
DATE	10-10-1988	10-10-1988	10-10-1988	10-10-1988	10-10-1988
UNCLASSIFIED	1	2	3	4	5

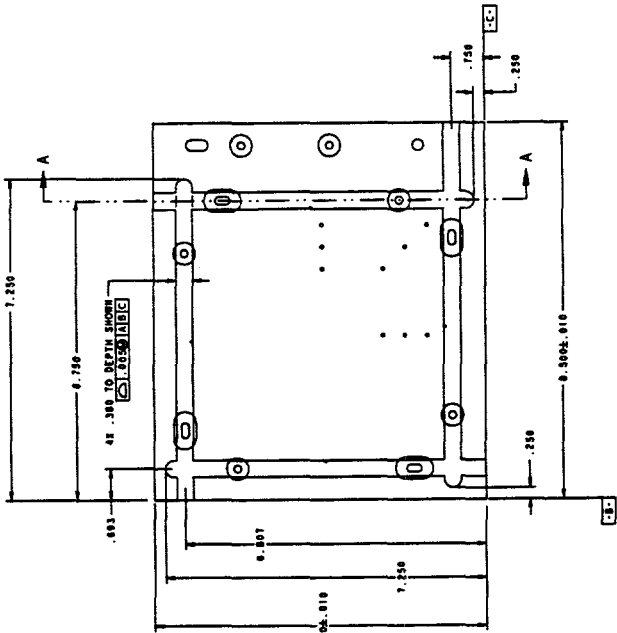
UNCLASSIFIED

NOTES:
1. GENERAL REQUIREMENTS PER 6000000.
2. MATERIAL: MARANTITE, 1.00 TON.

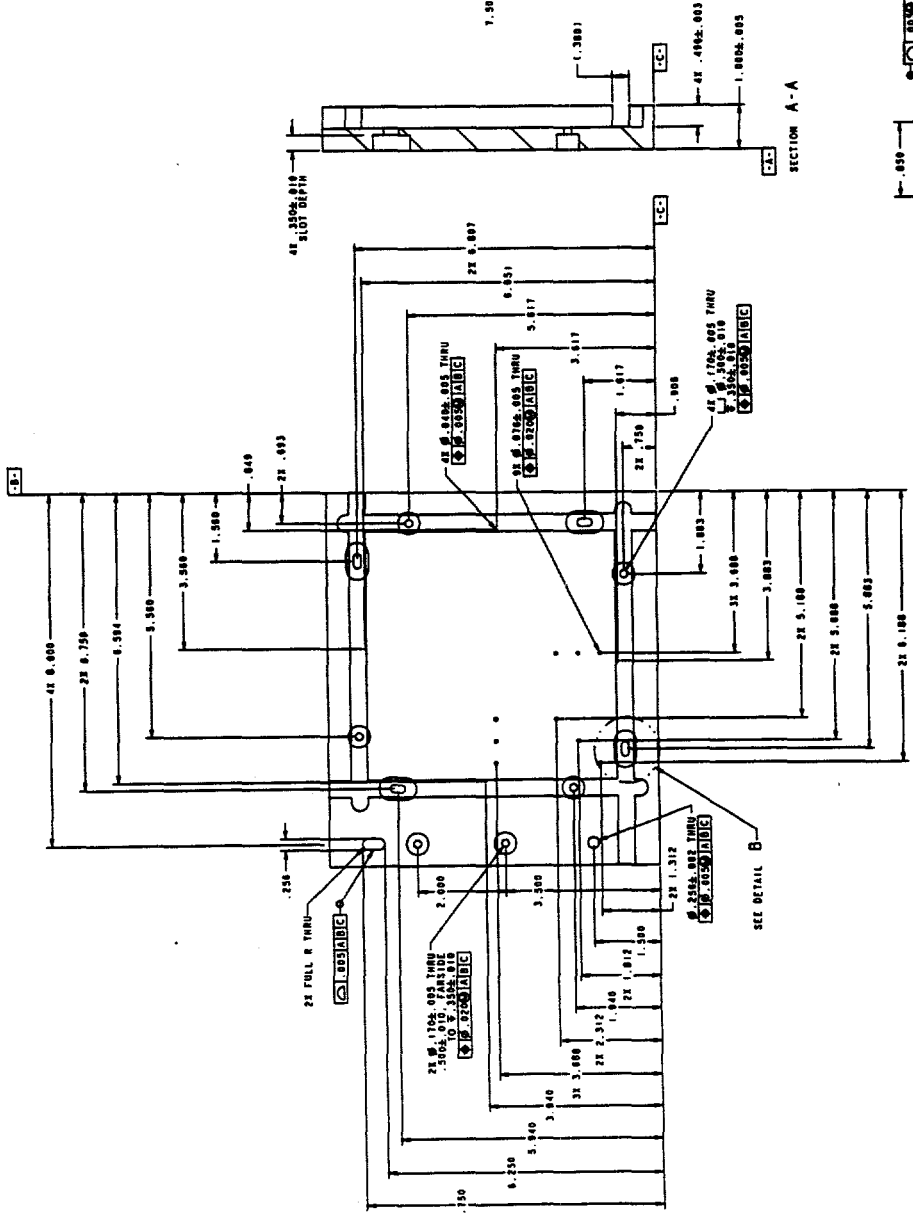
SEARCHED	INDEXED								
NAME	NUMBER								
ROBERTSON, GENE	851213-000								



SCALE 1.000



-A-



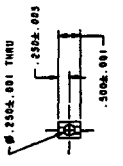
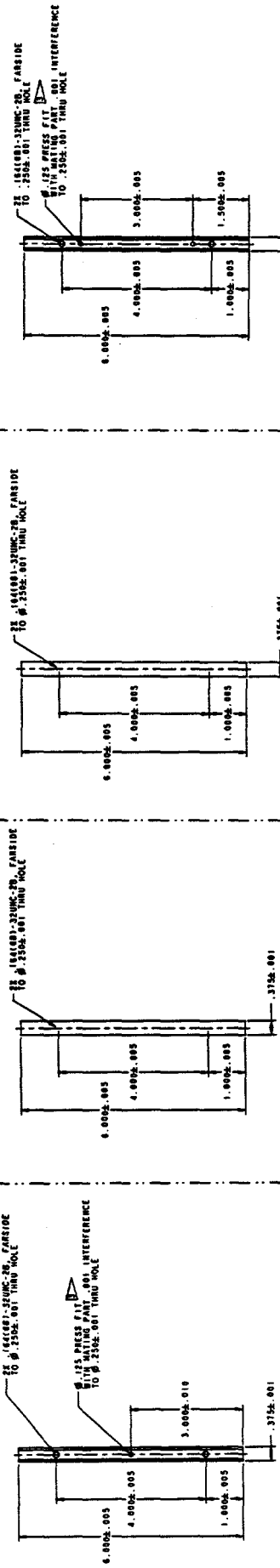
DETAILED
SCALE 1:250,000

UNCLASSIFIED

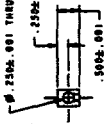
NOTE:

- GENERAL REQUIREMENTS PER DRAWING.
- MATERIAL: ALUMINUM, 6061-T6.
- POLE 1 AND 2 PRESS FIT WITH INTERFERENCE, 10 μ IN. ALUMINUM, CLASS 10K, 1000.

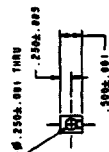
PART NUMBER	NAME	DESCRIPTION	SIZE	CLASS	DRAW	REV.	REVISION
			10	10	10	10	
SEE TABULATION	X	WIRELINE 7103 /					P03



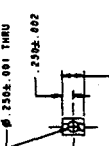
R51429-004



R51429-003



R51429-002



R51429-001

PART NUMBER	PART CLASSIFICATION	LINE				
		1	2	3	4	5
R51429-001	UNCLASSIFIED					
R51429-002	UNCLASSIFIED					
R51429-003	UNCLASSIFIED					
R51429-004	UNCLASSIFIED					

PART NUMBER	PART CLASSIFICATION	LINE				
		1	2	3	4	5
R51429-001	HOLDER, HEATER, BOTTOM (U)					
R51429-002	HOLDER, HEATER, BOTTOM (U)					
R51429-003	HOLDER, HEATER, BOTTOM (U)					
R51429-004	HOLDER, HEATER, BOTTOM (U)					

DRAWING NO. 51429-001-001 REV. B

DATE 01-20-77

DRAFTED BY J. BROWN

CHECKED BY J. BROWN

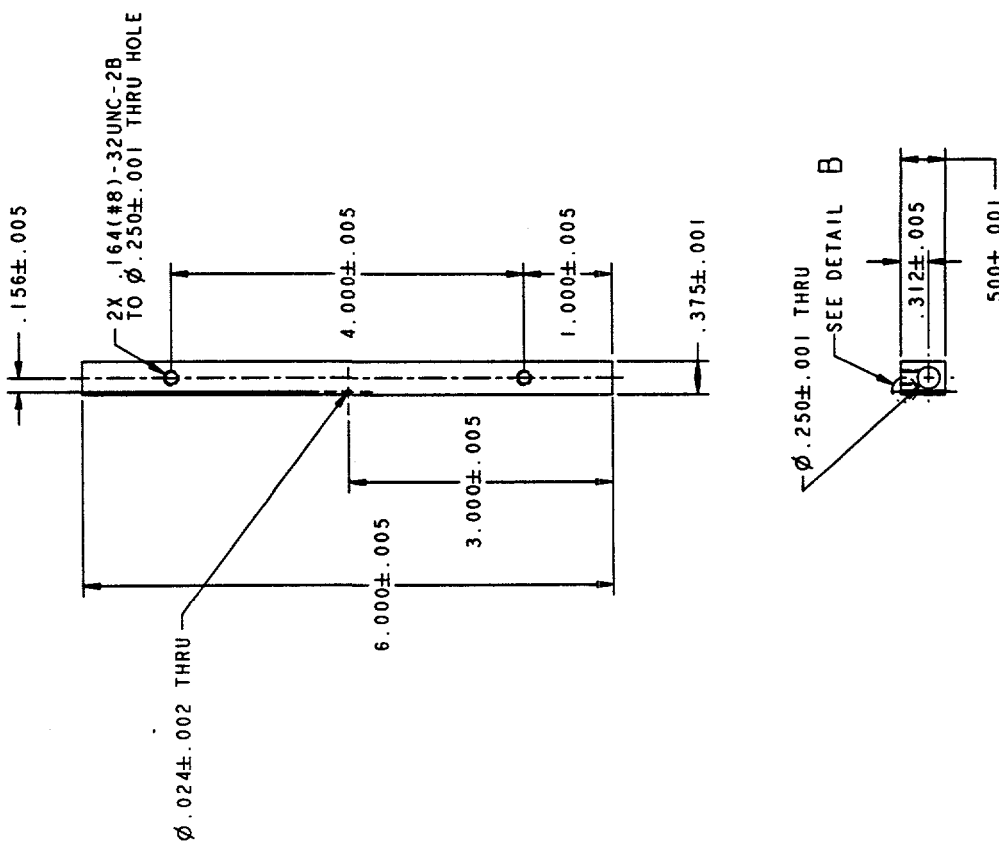
APPROVED BY J. BROWN

UNCLASSIFIED 4

NOTES:

1. GENERAL REQUIREMENTS PER 9900000.
2. MATERIAL: ALUMINUM, 6061-T6.

DESIGN AGENCY		PREPARED BY		REVISIONS	
PART NUMBER		SHEET ZONE		DESCRIPTION	
R51430-000		A		T. WISELEY, 9/183 / T. STRÖMBERG, 11/84	
PCS		DATE	CNR	APVB	



SHEET	1	2	3	4	5	6	7	8	9	10	11	12	13	14	15	16	17	18	19	20
ISSUE	A																			
PART CLASSIFICATION																				
UNCLASSIFIED																				
DRAWING CLASSIFICATION																				
UNCLASSIFIED																				
DRAWING NUMBER	C	R51430																		
SCALE	1:000	1:000	1:000	1:000	1:000	1:000	1:000	1:000	1:000	1:000	1:000	1:000	1:000	1:000	1:000	1:000	1:000	1:000	1:000	
DETAIL	B																			
SCALE	5.000																			

UNCLASSIFIED 4

NOTES:

1. GENERAL REQUIREMENTS PER 99000000.

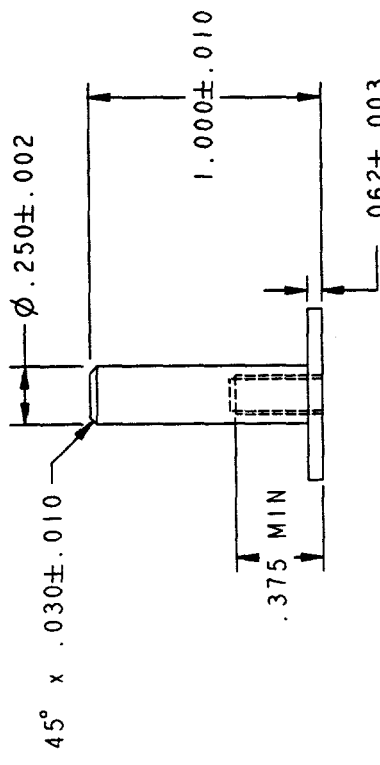
2. MATERIAL: SS 304.

3

2

1

REVISIONS					
DESIGN AGENCY	PART NUMBER	ISS	SHEET	PREPARED BY	DESCRIPTION
R51431-000	A	T. WISELEY	9783 /	P. STROMBERG, 1484	PGS



$\phi .740 \pm .005$ ← 1.64 (#8) - 32UNC-2B
TO DEPTH SHOWN, MINIMUM

C

B

C

B

SHEET 1 2 3 4 5 6 TITLE PIN, ALIGNMENT, PLATES
ISSUE A

PART CLASSIFICATION UNCLASSIFIED
DRAWING CLASSIFICATION UNCLASSIFIED

SIZE DRAWING NUMBER
B R51431
CAGEC 14213

SCALE 2.000 SHEET 1 OF 1
ORIGIN SA-PRO-17.0

GEOMETRIC PRECISION = XX.XXX XXX XXX

3

2

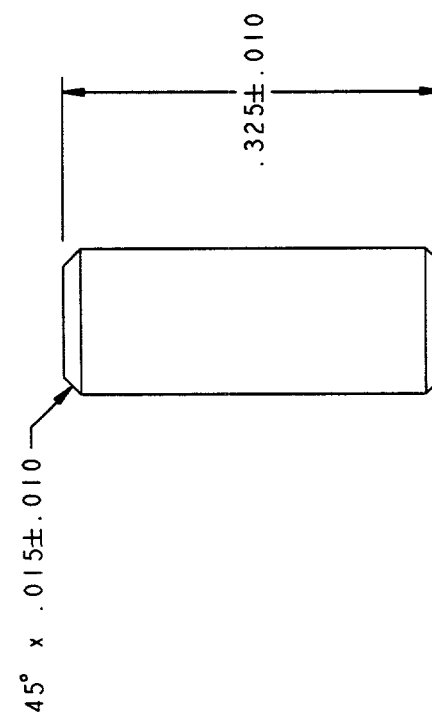
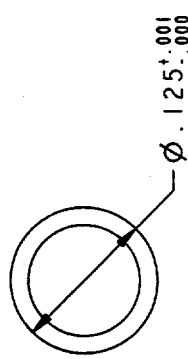
1

A

A

UNCLASSIFIED 4

NOTES:
1. GENERAL REQUIREMENTS PER 99000000.
2. MATERIAL: SS 304.



DESIGN AGENCY		REVISIONS			
PART NUMBER	ISSUE	SHEET	ZONE	PREPARED BY	DESCRIPTION
R51-432-000	A			T. WISELEY, 9783 / P. STROMBERG, 1484	

SHEET	1	2	3	4	5	6	TITLE	PIN, ALIGNMENT, GLASS
ISSUE	A							(U) (GOLDEN PHOTON)
PART CLASSIFICATION								
UNCLASSIFIED								
DRAWING CLASSIFICATION							SIZE	DRAWING NUMBER
UNCLASSIFIED							B	R51432
							CAGEC 14213	SCALE 0.000 SHEET 1 OF 1
STATUS	SA-REL-4-Sep-96						ORIGIN	SA-PRO-17.0

GEOMETRIC PRECISION = XX.XXX XXX XX

2

A

1

UNCLASSIFIED

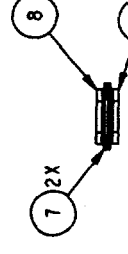
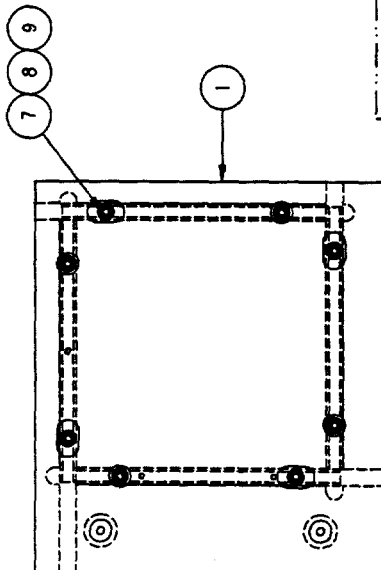
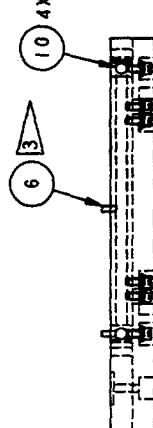
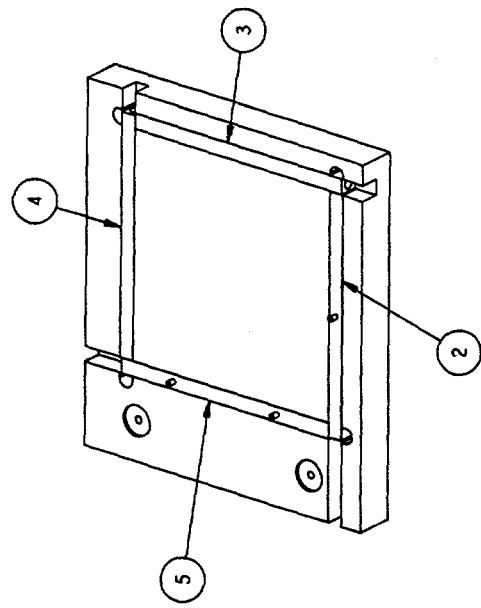
11070

1. MAY BE OBTAINED FROM: WATLOW CONTROLS,
1241 BUNDY BLVD, WINONA MN 55987-5580.
PHONE 507-454-5300 OR FAX 507-452-4507
OR FROM CONNECTING COMPONENTS, A DIV. OF TMA, INC
6800 ACADEMY PARKWAY WEST NE, ALBUQUERQUE,
NM 87109. PHONE 505-345-8921.

2. MAY BE OBTAINED FROM: W M BERG, INC
499 OCEAN AVE, EAST ROCKAWAY NY 11518.
PHONE 516-596-1700 FAX 516-599-3274.

PRESS FIT 001 INTERFERENCE FIT

31



1. TYPICAL WASHER

ECONOMIC REGRESSION: NOV.

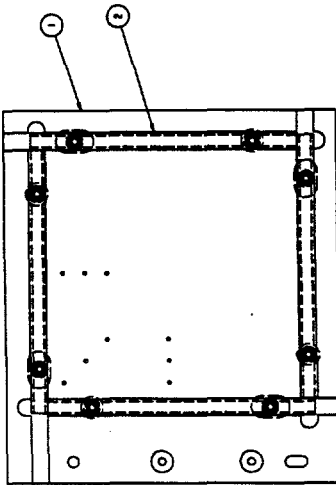
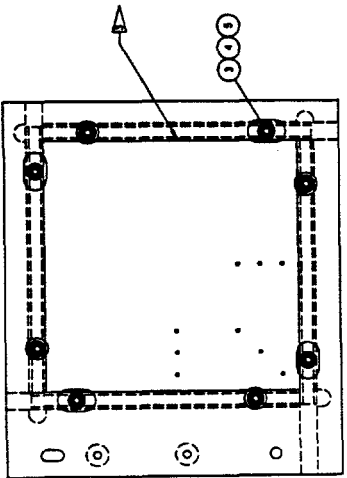
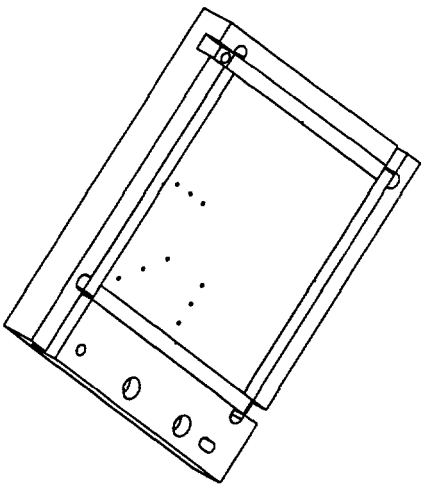
UNCLASSIFIED

NOTES:

1. MAY BE CONTAINED FROM: WATLOW CONTROLS,
1414 BURG WY, WATLOW, MO 64086-1300,
C/O FEDERAL INDUSTRIAL CONTROLS, INC.
800 ACADIA PARKWAY WEST, ALBUQUERQUE,
NM 87123-900.
2. MAY BE CONTAINED FROM: WATLOW,
1414 BURG WY, WATLOW, MO 64086-1300,
C/O FEDERAL INDUSTRIAL CONTROLS, INC.
800 ACADIA PARKWAY WEST, ALBUQUERQUE,
NM 87123-900.

VERITY THAT HOLES FOR THERMOCOUPLES ARE
ALIGNED TOWARD THE FRONT SIDE OF THE
WATER HEATER.

part number	description	unit	count	supp
9517327-000	WATER HEATER, STAINLESS STEEL, 24" X 36"	PC	1	



TYPICAL WASHER
ASSEMBLY

part number	description	unit	count	supp
4 050-6	WATER, 24" X 36" STAINLESS STEEL TANK	PC	1	
10 051-1	FLANGE, BELLEVILLE, 10" ID - 315 LB	PC	1	
10 04525-0	FLANGE, BELLEVILLE, 10" ID - 315 LB	PC	1	
8 051-511-31	SCREW, SET IN CAP - STAINLESS STEEL, 2 - 315 LB	PC	2	
4 051-512-000	WRENCH, WHEEL, TOP	PC	1	
1 051-520-000	PLATE, TOP	PC	1	

part number	description	unit	count	supp
4 051-6	WATER, 24" X 36" STAINLESS STEEL TANK	PC	1	
10 051-1	FLANGE, BELLEVILLE, 10" ID - 315 LB	PC	1	
10 04525-0	FLANGE, BELLEVILLE, 10" ID - 315 LB	PC	1	
8 051-511-31	SCREW, SET IN CAP - STAINLESS STEEL, 2 - 315 LB	PC	2	
4 051-512-000	WRENCH, WHEEL, TOP	PC	1	
1 051-520-000	PLATE, TOP	PC	1	

UNCLASSIFIED

3

2

1

NOTES:

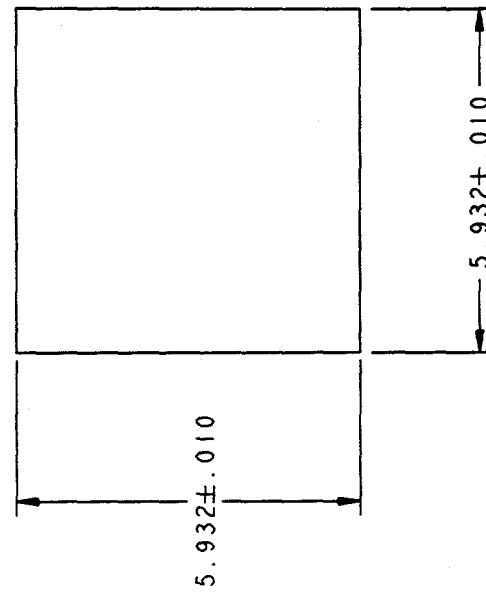
1. GENERAL REQUIREMENTS PER 9900000.
2. MATERIAL: GLASS.

REVISIONS					
DESIGN AGENCY	PART NUMBER	ISSUE	SHEET	PREPARED BY	DESCRIPTION
R51435-000	A			T. WISELEY, 9783 / P. STROMBERG, 1484	

D

C

D



C

B

B

.118±.002

SHEET	1	2	3	4	5	6	TITLE	GLASS, BOTTOM
ISSUE	A							(U) (GOLDEN PHOTON)
PART CLASSIFICATION								
UNCLASSIFIED								
DRAWING CLASSIFICATION								
UNCLASSIFIED								
SIZE								
B	R51435							
COGEC 14213								
SCALE 0.500								
SHEET 1 OF 1								
ORIGIN SA-PRO-17.0								

STATUS SA-REL-4-Sep-96

2

GEOMETRIC PRECISION = XX.XXX XXX XX

1

A

C

A

UNCLASSIFIED 4

NOTES:

1. GENERAL REQUIREMENTS PER 9900000.
2. MATERIAL: GLASS.

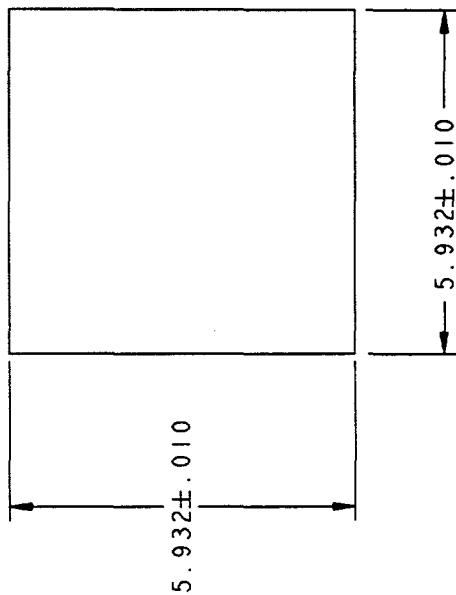
NOTES:		REVISIONS							
		ISSUE	SHEET	ZONE	PREPARED BY	DESCRIPTION	DATE	CHNR	APVO
D		A	R51436-000	A	T. WISELEY / P. STROMBERG, 1484				PGS

D

C

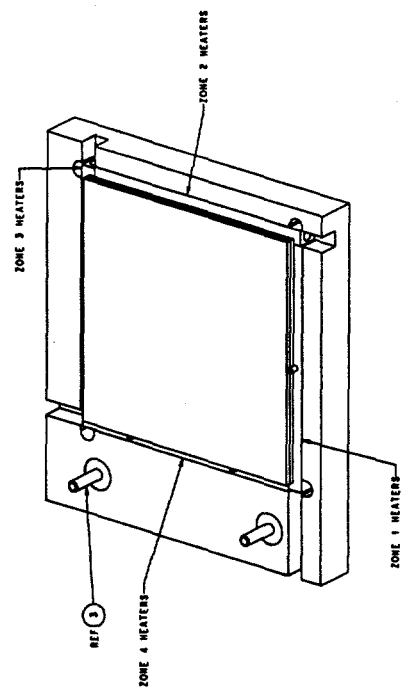
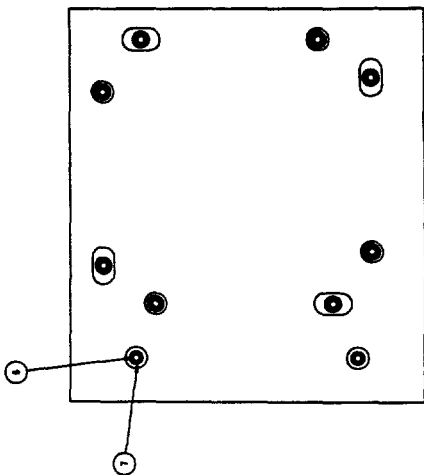
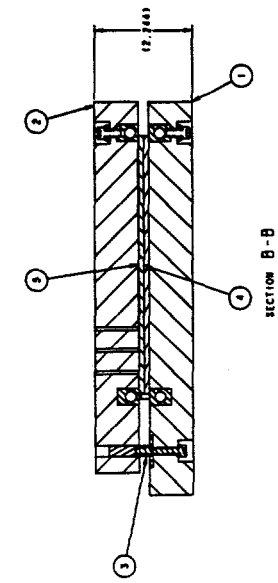
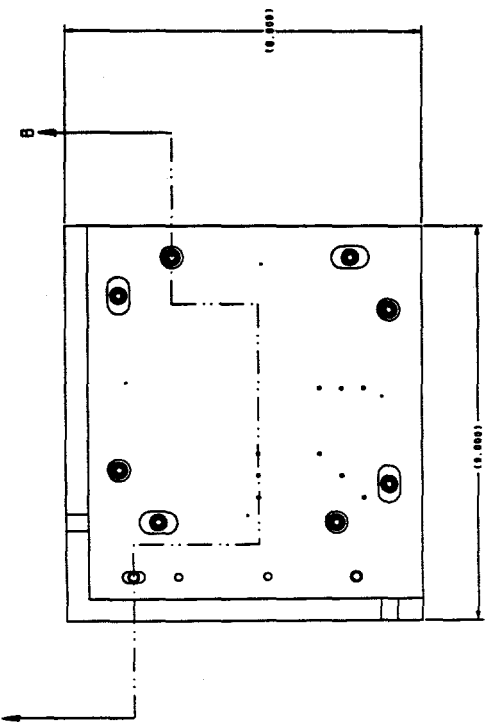
B

A



SHEET	1	2	3	4	5	6	TITLE	GLASS,			
	ISSUE	A						TOP			
PART CLASSIFICATION		UNCLASSIFIED					(U) (GOLDEN PHOTON)				
DRAWING CLASSIFICATION		UNCLASSIFIED					SIZE DRAWING NUMBER				
DRAWING CLASSIFICATION		B					R51436				
DRAWING CLASSIFICATION		B					CAGEC 14213				
DRAWING CLASSIFICATION		B					SCALE 0.500				
DRAWING CLASSIFICATION		B					SHEET 1 OF 1				
DRAWING CLASSIFICATION		B					ORIGIN SA-PRO-17.0				
DRAWING CLASSIFICATION		B					1				
DRAWING CLASSIFICATION		B					2				
DRAWING CLASSIFICATION		B					3				
DRAWING CLASSIFICATION		B					A				
DRAWING CLASSIFICATION		B					1				
DRAWING CLASSIFICATION		B					2				
DRAWING CLASSIFICATION		B					3				
DRAWING CLASSIFICATION		B					A				
DRAWING CLASSIFICATION		B					1				
DRAWING CLASSIFICATION		B					2				
DRAWING CLASSIFICATION		B					3				
DRAWING CLASSIFICATION		B					A				
DRAWING CLASSIFICATION		B					1				
DRAWING CLASSIFICATION		B					2				
DRAWING CLASSIFICATION		B					3				
DRAWING CLASSIFICATION		B					A				
DRAWING CLASSIFICATION		B					1				
DRAWING CLASSIFICATION		B					2				
DRAWING CLASSIFICATION		B					3				
DRAWING CLASSIFICATION		B					A				
DRAWING CLASSIFICATION		B					1				
DRAWING CLASSIFICATION		B					2				
DRAWING CLASSIFICATION		B					3				
DRAWING CLASSIFICATION		B					A				
DRAWING CLASSIFICATION		B					1				
DRAWING CLASSIFICATION		B					2				
DRAWING CLASSIFICATION		B					3				
DRAWING CLASSIFICATION		B					A				
DRAWING CLASSIFICATION		B					1				
DRAWING CLASSIFICATION		B					2				
DRAWING CLASSIFICATION		B					3				
DRAWING CLASSIFICATION		B					A				
DRAWING CLASSIFICATION		B					1				
DRAWING CLASSIFICATION		B					2				
DRAWING CLASSIFICATION		B					3				
DRAWING CLASSIFICATION		B					A				
DRAWING CLASSIFICATION		B					1				
DRAWING CLASSIFICATION		B					2				
DRAWING CLASSIFICATION		B					3				
DRAWING CLASSIFICATION		B					A				
DRAWING CLASSIFICATION		B					1				
DRAWING CLASSIFICATION		B					2				
DRAWING CLASSIFICATION		B					3				
DRAWING CLASSIFICATION		B					A				
DRAWING CLASSIFICATION		B					1				
DRAWING CLASSIFICATION		B					2				
DRAWING CLASSIFICATION		B					3				
DRAWING CLASSIFICATION		B					A				
DRAWING CLASSIFICATION		B					1				
DRAWING CLASSIFICATION		B					2				
DRAWING CLASSIFICATION		B					3				
DRAWING CLASSIFICATION		B					A				
DRAWING CLASSIFICATION		B					1				
DRAWING CLASSIFICATION		B					2				
DRAWING CLASSIFICATION		B					3				
DRAWING CLASSIFICATION		B					A				
DRAWING CLASSIFICATION		B					1				
DRAWING CLASSIFICATION		B					2				
DRAWING CLASSIFICATION		B					3				
DRAWING CLASSIFICATION		B					A				
DRAWING CLASSIFICATION		B					1				
DRAWING CLASSIFICATION		B					2				
DRAWING CLASSIFICATION		B					3				
DRAWING CLASSIFICATION		B					A				
DRAWING CLASSIFICATION		B					1				
DRAWING CLASSIFICATION		B					2				
DRAWING CLASSIFICATION		B					3				
DRAWING CLASSIFICATION		B					A				
DRAWING CLASSIFICATION		B					1				
DRAWING CLASSIFICATION		B					2				
DRAWING CLASSIFICATION		B					3				
DRAWING CLASSIFICATION		B					A				
DRAWING CLASSIFICATION		B					1				
DRAWING CLASSIFICATION		B					2				
DRAWING CLASSIFICATION		B					3				
DRAWING CLASSIFICATION		B					A				
DRAWING CLASSIFICATION		B					1				
DRAWING CLASSIFICATION		B					2				
DRAWING CLASSIFICATION		B					3				
DRAWING CLASSIFICATION		B					A				
DRAWING CLASSIFICATION		B					1				
DRAWING CLASSIFICATION		B					2				
DRAWING CLASSIFICATION		B					3				

UNCLASSIFIED



ITEM 3 SCALING

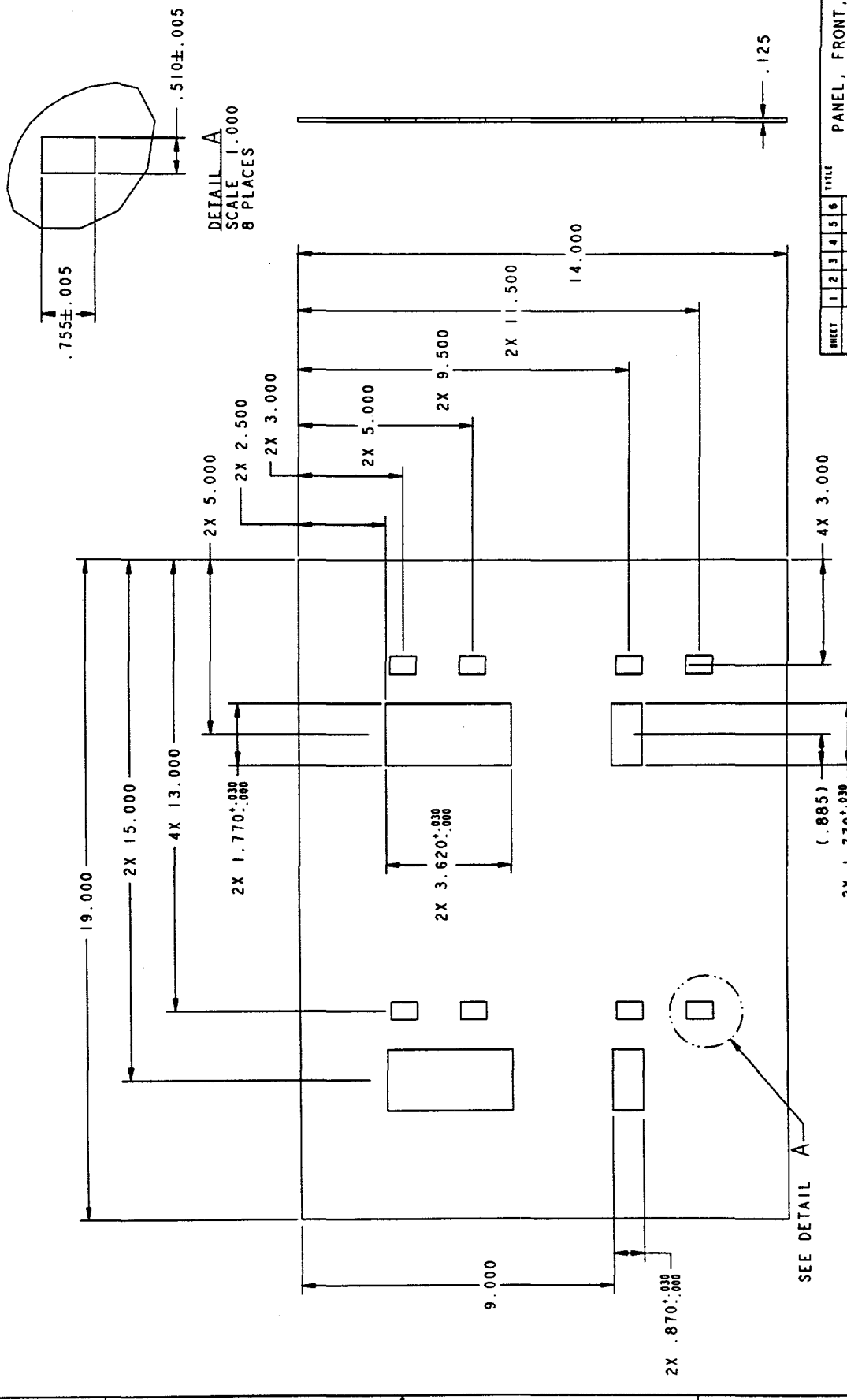
UNCLASSIFIED 4

NOTES:

1. GENERAL REQUIREMENTS PER 9900000.

2. MAY BE OBTAINED FROM: ALLIED ELECTRONICS,
7410 PEBBLE DRIVE FORT WORTH, TX 76118
800-433-5700 OR 505-266-7565
STOCK #806-4020/ MFR'S #PBA19014CG2.

DESIGN ARTICLE		REVISIONS	
PART NUMBER	ISSUE	PREPARED BY	DESCRIPTION
RS1438-000	A	T. W. SELEY 9/83 / P. STRONBERG 1-84	DATE CHNR APWD PQS



SHEET		1	2	3	4	5	6	TITLE	
ISSUE	A							(U) (GOLDEN PHOTON)	
PART CLASSIFICATION	UNCLASSIFIED		DRAWING CLASSIFICATION		DRAWING NUMBER		SIZE		
UNCLASSIFIED	C		RS1438		C4213		SCALE 0.500		
STATUS	SA-REF-A-Rev-98		C4213		SA-PRO-17.0		SHEET 1 OF 1		

UNCLASSIFIED

177

6

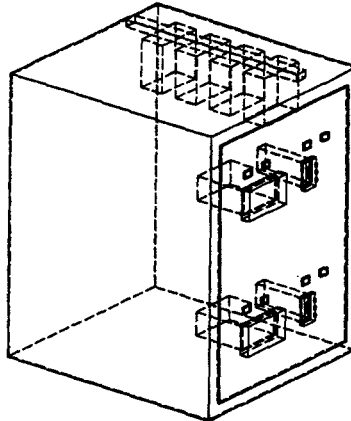
6

1

1

DESIGN AGENCY PART NUMBER		REVISIONS		PREPARED BY	
		155 SHEET ZONE			
R54350-000		A		T. WISELEY	
				9783	

A schematic diagram of a control panel. It features two sets of indicator lights, each consisting of two small squares arranged in a cross pattern. Between these two sets of lights is a larger rectangular component. The entire assembly is enclosed in a rectangular frame.



REVISIONS					
ISS	SHEET	PREPARED BY	DESCRIPTION	DATE	CHNR
ZONE					AFVD
A		T. WISER/MEG	9783 / P. STRONBERG 2334		ccc

GEOMETRIC PRECISION = XXX.XXX XXX XXX XXX

1

Distribution:

- 5 Golden Genesis Co.
Attn: J. Michael Davis
4595 McIntyre St.
Golden, CO 80403
- 2 Global Solar Energy
Attn: Scot Albright
12401 W. 49th Ave.
Wheat Ridge, CO 80033
- 1 Golden Photon
Attn: Gail Constancio
PO Box 4040
Golden, CO 80402

- 1 MS 0367 B. K. Damkroger, 1833
- 6 0367 S. J. Glass, 1833
- 2 0443 E. L. Hoffman, 9117
- 1 0443 H. S. Morgan, 9117
- 1 0455 M. L. Tatro, 6231
- 2 0501 P. G. Stromberg, 2334
- 2 0710 P. M. Baca, 1845
- 1 0752 D. L. King, 6219
- 1 0752 M. A. Quintana, 6219
- 2 0835 S. E. Gianoulakis, 9113
- 1 0835 S. N. Kempka, 9113
- 2 0835 T. E. Voth, 9113
- 1 0873 L. Kovacic, 143022
- 2 0958 R. R. Dubois, 1484
- 1 0959 F. P. Gerstle, 1492
- 2 0959 S. T. Reed, 1492
- 2 1349 W. F. Hammetter, 1846
- 1 1349 R. E. Loehman, 1800
- 2 1411 F. M. Hosking, 1833
- 1 1434 G. E. Pike, 1802
- 1 1435 D. E. Arvizu, 1800

- 1 MS 9018 Central Technical Files, 8940-2
- 2 0899 Technical Library, 4916
- 2 0619 Review & Approval Desk, 12690
For DOE/OSTI
- 1 1380 Technology Transfer, 4212